

TECHNICAL REPORT ARLCB-TR-77047

COLLAPSED 12-NODE TRIANGULAR ELEMENTS AS CRACK  
TIP ELEMENTS FOR ELASTIC FRACTURE

S.L. Pu  
M.A. Hussain  
W.E. Lorensen

TECHNICAL  
LIBRARY

December 1977



US ARMY ARMAMENT RESEARCH AND DEVELOPMENT COMMAND  
LARGE CALIBER WEAPON SYSTEMS LABORATORY  
BENÉ WEAPONS LABORATORY  
WATERVLIET, N. Y. 12189

AMCMS No. 611102.H54001

PRON No. 1A-7-51701-(02)-M7

APPROVED FOR PUBLIC RELEASE; DISTRIBUTION UNLIMITED

#### DISCLAIMER

The findings in this report are not to be construed as an official Department of the Army position unless so designated by other authorized documents.

The use of trade name(s) and/or manufacturer(s) does not constitute an official indorsement or approval.

#### DISPOSITION

Destroy this report when it is no longer needed. Do not return it to the originator.

REPORT DOCUMENTATION PAGE		READ INSTRUCTIONS BEFORE COMPLETING FORM
1. REPORT NUMBER ARLCB-TR-77047	2. GOVT ACCESSION NO.	3. RECIPIENT'S CATALOG NUMBER
4. TITLE (and Subtitle) COLLAPSED 12-NODE TRIANGULAR ELEMENTS AS CRACK TIP ELEMENTS FOR ELASTIC FRACTURE		5. TYPE OF REPORT & PERIOD COVERED
		6. PERFORMING ORG. REPORT NUMBER
7. AUTHOR(s) S.L PU M.A HUSSAIN W.E. LORENSEN		8. CONTRACT OR GRANT NUMBER(s)
9. PERFORMING ORGANIZATION NAME AND ADDRESS Benet Weapons Laboratory Watervliet Arsenal, Watervliet, N.Y. 12189 DRDAR- <u>LCB</u> -RA		10. PROGRAM ELEMENT, PROJECT, TASK AREA & WORK UNIT NUMBERS AMCMS No. 611102.H54001 PRON No. 1A-7-51701-(02)-M7
11. CONTROLLING OFFICE NAME AND ADDRESS Us. Army Armament Research and Development Command Large Caliber Weapon Systems Laboratory Dover, New Jersey 07081		12. REPORT DATE December 1977
		13. NUMBER OF PAGES 49
14. MONITORING AGENCY NAME & ADDRESS (if different from Controlling Office)		15. SECURITY CLASS. (of this report) UNCLASSIFIED
		15a. DECLASSIFICATION/DOWNGRADING SCHEDULE
16. DISTRIBUTION STATEMENT (of this Report)  Approved for public release; distribution unlimited.		
17. DISTRIBUTION STATEMENT (of the abstract entered in Block 20, if different from Report)		
18. SUPPLEMENTARY NOTES		
19. KEY WORDS (Continue on reverse side if necessary and identify by block number) Fracture Mechanics      Finite-Element Method      Cubic, quadrilateral Elements  Isoparametric Elements      Singular Elements      Stress intensity Factors		
20. ABSTRACT (Continue on reverse side if necessary and identify by block number) For the 12-node bicubic, quadrilateral, isoparametric elements, it is shown that the inverse square root singularity of the strain field at the crack tip can be obtained by the simple technique of collapsing the quadrilateral elements into triangular elements around the crack tip and placing the two mid-side nodes of each side of the triangles at 1/9 and 4/9 of the length of the side from the tip. This is analgous to placing the mid-side nodes at quarter points in the (See Other Side)		

Block No. 20.

vicinity of the crack tip for the quadratic, isoparametric element.

The advantage of this method are that the displacement compatibility is satisfied throughout the region and that there is no need of special crack tip elements. The stress intensity factors can be accurately obtained by using general purpose programs having isoparametric elements such as NASTRAN. The use of 12-node isoparametric element program APES may be simplified by eliminating the special crack tip elements.

## TABLE OF CONTENTS

	<u>Page</u>
INTRODUCTION	1
THE 12-NODE QUADRILATERAL ISOPARAMETRIC ELEMENT	3
THE CRACK TIP ELEMENT	6
DETERMINATION OF STRESS INTENSITY FACTORS	12
1. One Term Expansion	14
2. Two-Term Expansion	15
3. Four Term Expansion	16
4. Collocation Method	16
NASTRAN IMPLEMENTATION	17
NUMERICAL RESULTS	18
THE STABILITY OF COLLAPSED TRIANGULAR ELEMENTS	33
CONCLUSIONS	35
REFERENCES	36

### ILLUSTRATIONS

1. Shape Functions and Numbering Sequence for a 12-Node Quadrilateral Element.	39
2. A Normalized Square in $(\xi, \eta)$ Plane Mapped Into a Collapsed Triangular Element in $(x, y)$ Plane with the side $\xi = -1$ Degenerated into a Point at the Crack Tip.	40
3. Three Tension Test Specimens.	41
4. Idealization of a Half of the Single-Edge Cracked Tension Specimen.	42

	<u>Page</u>
5. (a) Three Collapsed Triangular Elements Surrounding a Mode I Crack Tip.	43
(b) Special Core Element and Three Quadrilateral Elements Surrounding a Mode I Crack Tip.	43
6. (a) Six Collapsed Triangular Elements Surrounding a Mixed Mode Crack Tip.	44
(b) Special Core Element and Six Quadrilateral Elements Surrounding a Moxed Mode Crack Tip.	44
7. Idealization of a 45-Degree Slant Edge Cracked Panel in Tension.	45
8. (a) Node 5 Perturbed to 5*.	46
(b) Nodes 20, 21, 23, 24, 26, 27 Perturbed From Their Nominal Positions.	46

#### TABLES

1. RATIOS OF $K_I$ (APES) TO $K_I$ (EXACT)	21
2. $K_I$ (FINITE ELEMENT)/ $K_I$ (EXACT) BY ONE-TERM EXPANSION USING APES WITH COLLAPSED TRIANGULAR ELEMENTS	22
3. $K_I$ (FINITE ELEMENT)/ $K_I$ (EXACT) BY ONE-TERM EXPANSION USING APES WITH COLLAPSED TRIANGULAR ELEMENTS	23
4. $K_I$ (FINITE ELEMENT)/ $K_I$ (EXACT) BY ONE-TERM EXPANSION USING APES WITH COLLAPSED TRIANGULAR ELEMENTS	24
5. $K_I$ (FINITE ELEMENT)/ $K_I$ (EXACT) BY TWO-TERM EXPANSION USING APES WITH COLLAPSED TRIANGULAR ELEMENTS	25
6. $K_I$ (FINITE ELEMENT)/ $K_I$ (EXACT) BY TWO-TERM EXPANSION USING APES WITH COLLAPSED TRIANGULAR ELEMENTS	26
7. $K_I$ (FINITE ELEMENT)/ $K_I$ (EXACT) BY TWO-TERM EXPANSION USING APES WITH COLLAPSED TRIANGULAR ELEMENTS	27
8. $\frac{K_I \text{ (FINITE ELEMENT)}}{K_I \text{ (EXACT)}}$ BY FOUR-TERM EXPANSION USING APES WITH COLLAPSED TRIANGULAR ELEMENTS	28

	<u>Page</u>
9. $K_1$ (FINITE ELEMENT) FOR SINGLE EDGE CRACK USING COLLOCATION METHOD. NODAL DISPLACEMENTS OBTAINED FROM APES WITH 3-COLLAPSED TRIANGULAR ELEMENTS. COLLOCATION POINTS ARE EQUALLY SPACED ON $r=0.01$ .	29
10. $K_1$ (NASTRAN)/ $K_1$ (EXACT)	30
11. $K_1$ (APES)/ $K_1$ (EXACT)	31
12. $K_1$ AND $K_2$ FOR $45^\circ$ EDGE CRACK BY NASTRAN	33

## INTRODUCTION

The direct application of the finite element method to crack problems was studied by a number of investigators [1-3]. No special attention was given to the singular nature of stress and strain of a crack tip. Because of the large strain gradients in the vicinity of a crack tip, it requires the use of an extremely fine element grid near the crack tip. By comparing the finite element result of displacement components or stress components at a nodal point with the corresponding asymptotic result of displacement or stress components at that node, the stress intensity factor can be estimated. The estimated values of a stress intensity factor vary over a considerable range, depending on which node is taken for computation. This results in poor estimates if displacements are taken at nodal points either very close to or far away from the crack tip.

An improved finite element technique was developed by Wilson [4]. It combined the asymptotic expansion of displacements in a small circular core region surrounding a crack tip and the finite element approximation outside a polygon approximating the circular arc of the

---

<sup>1</sup>Swedlow, J. L., Williams, M. L., and Yang, W. H., "Elasto-Plastic Stresses and Strains in Cracked Plates," Proceedings First International Conference on Fracture, 1, p. 259, 1966.

<sup>2</sup>Kobayashi, A. S., Maiden, D. E. and Simon, B. J., "Application of the Method of Finite Element Analysis to Two-Dimensional Problems in Fracture Mechanics," ASME 69-WA/PVP-12 (1969).

<sup>3</sup>Chan, S. K., Tuba, I. S. and Wilson, W. K., "On Finite Element Method in Linear Fracture Mechanics," Engineering Fracture Mechanics, 2, p. 1, 1970.

<sup>4</sup>Wilson, W. K., "Combined Mode Fracture Mechanics," Ph.D. Dissertation, University of Pittsburgh, 1969.



core region. The displacement fields obtained from these two approximations are not, in general, continuous along the asymptotic expansion-finite element interface except at discrete nodal points.

An alternative finite element approach to crack problems is the use of special elements in the region of the crack tip, e.g. [5-7]. In [5], Tracey employs quadrilateral isoparametric elements which become triangular around the crack tip. The displacement functions of the two types of elements are selected such that displacements are continuous everywhere, and the near tip displacements are proportional to the square root of the distance from the crack tip.

Henshell and Shaw [8] and Barsoum [9] showed that special crack tip elements were unnecessary. For two-dimensional 8-node quadrilateral elements, the inverse square root singularity of the strain field at the crack tip is obtained by collapsing quadrilateral elements into triangular elements and placing the mid-side nodes at quarter points

---

<sup>5</sup>Tracey, D. M., "Finite Elements for Determination of Crack Tip Elastic Stress Intensity Factors," Engineering Fracture Mechanics, Vol. 3, 1971.

<sup>6</sup>Blackburn, W. S., "Calculation of Stress Intensity Factors at Crack Tips Using Special Finite Elements," The Mathematics of Finite Elements and Applications, Brunel University, 1973.

<sup>7</sup>Benzley, S. E. and Beisinger, A. E., "Chiles - A Finite Element Computer Program that Calculates the Intensities of Linear Elastic Singularities," Sandia Laboratories, Technical Report SLA-73-0894, 1973.

<sup>8</sup>Henshell, R. D., and Shaw, K. G., "Crack Tip Finite Elements Are Unnecessary," International Journal for Numerical Methods in Engineering, Vol. 10, 1975.

<sup>9</sup>Barsoum, R. S., "On the Use of Isoparametric Finite Elements in Linear Fracture Mechanics," International Journal for Numerical Methods in Engineering, Vol. 10, 1976.

from the tip. The quarter-point quadratic isoparametric elements, as singular elements for crack problems, have been implemented in NASTRAN by Hussain et al [10].

In order to reduce the computer core requirement and to simplify the modeling of a structure, better known but lower order finite elements have been abandoned in favor of cubic 12-node, isoparametric, quadrilateral elements as described by Zienkiewicz [11]. In this paper, the concept of quarter-point, quadratic, isoparametric elements is extended to 12-node cubic isoparametric elements. The correct order of strain singularity at the crack tip is achieved in a simple manner by collapsing the quadrilateral elements into triangular elements and by placing the two middle nodes of a side at  $1/9$  and  $4/9$  of the length of the side from the tip. The 12-node, isoparametric elements have been implemented in NASTRAN. Both mode I and mixed mode crack problems are computed by NASTRAN using the collapsed elements to assess the accuracy. The stability of results is discussed when the collapsed triangular elements are used.

#### THE 12-NODE QUADRILATERAL ISOPARAMETRIC ELEMENT

A typical 12-node, quadrilateral element in Cartesian coordinates  $(x,y)$  which is mapped to a square in the curvilinear space  $(\xi,\eta)$  with vertices at  $(\pm 1, \pm 1)$  is shown in Figure 1. The assumption for displacement components takes the form:

<sup>10</sup>Hussain, M. A., Lorensen, W. E., and Pflagl, G., "The Quarter-Point Quadratic Isoparametric Element As a Singular Element for Crack Problems," NASA TM-X-3428, 1976, p. 419.

<sup>11</sup>Zienkiewicz, O. O., The Finite Element Method in Engineering Science, McGraw Hill, London, 1971.

$$\left. \begin{aligned} u &= \sum_{i=1}^{12} N_i(\xi, \eta) u_i \\ v &= \sum_{i=1}^{12} N_i(\xi, \eta) v_i \end{aligned} \right\} \quad (1)$$

where  $u, v$  are  $x, y$  components of displacement of a point whose natural coordinates are  $\xi, \eta$ ;  $u_i, v_i$  are displacement components of node  $i$  and  $N_i(\xi, \eta)$  is the shape function which is given by [11]

$$\begin{aligned} N_i(\xi, \eta) &= \frac{1}{256} (1 + \xi\xi_i)(1 + \eta\eta_i)[-10 + 9(\xi^2 + \eta^2)][-10 + 9(\xi_i^2 + \eta_i^2)] \\ &+ \frac{81}{256} (1 + \xi\xi_i)(1 + 9\eta\eta_i)(1 - \eta^2)(1 - \eta_i^2) \\ &+ \frac{81}{256} (1 + \eta\eta_i)(1 + 9\xi\xi_i)(1 - \xi^2)(1 - \xi_i^2) \end{aligned} \quad (2)$$

for node  $i$  whose Cartesian and curvilinear coordinates are  $(x_i, y_i)$  and  $(\xi_i, \eta_i)$  respectively. The details of the shape functions and the numbering sequence are given in Figure 1.

The same shape functions are used for the transformation of coordinates, hence the name isoparametric,

$$\left. \begin{aligned} x &= \sum_{i=1}^{12} N_i(\xi, \eta) x_i \\ y &= \sum_{i=1}^{12} N_i(\xi, \eta) y_i \end{aligned} \right\} \quad (3)$$

<sup>11</sup>Zienkiewicz, O.O., The Finite Element Method in Engineering Science, McGraw Hill, London, 1971.

The element stiffness matrix is found in the usual way and is given by [9,10]

$$[K] = \int_{-1}^1 \int_{-1}^1 [B]^T [D] [B] \det |J| d\xi d\eta \quad (4)$$

where [B] is a matrix relating joint displacements to strain field

$$[B] = [\dots B_i \dots], \quad [B_i] = \begin{bmatrix} \frac{\partial N_i}{\partial x} & 0 \\ 0 & \frac{\partial N_i}{\partial y} \\ \frac{\partial N_i}{\partial y} & \frac{\partial N_i}{\partial x} \end{bmatrix} \quad (5a)$$

and [D] is the material stiffness matrix and is given for the case of plane stress by

$$[D] = \frac{E}{1 - \nu^2} \begin{bmatrix} 1 & \nu & 0 \\ \nu & 1 & 0 \\ 0 & 0 & (1 - \nu)/2 \end{bmatrix} \quad (5b)$$

in which E is Young's modulus and  $\nu$  is Poisson's ratio.

The Jacobian matrix [J] is given by

<sup>9</sup>Barsoum, R. S., "On the Use of Isoparametric Finite Elements in Linear Fracture Mechanics," International Journal for Numerical Methods in Engineering, Vol. 10, 1976.

<sup>10</sup>Hussain, M. A., Lorensen, W. E., and Pflögl, G., "The Quarter-Point Quadratic Isoparametric Element as a Singular Element for Crack Problems," NASA TM-X-3428, 1976, p. 419.

$$[J] = \begin{bmatrix} \frac{\partial x}{\partial \xi} & \frac{\partial y}{\partial \xi} \\ \frac{\partial x}{\partial \eta} & \frac{\partial y}{\partial \eta} \end{bmatrix} = \begin{bmatrix} \dots & \frac{\partial N_j}{\partial \xi} & \dots \\ \dots & \frac{\partial N_j}{\partial \eta} & \dots \end{bmatrix} \begin{bmatrix} \cdot & \cdot \\ \cdot & \cdot \\ x_j & y_j \\ \cdot & \cdot \\ \cdot & \cdot \end{bmatrix} \quad (6)$$

whenever the determinant of  $[J]$  is zero, the stresses and strains become singular [8-10]. The derivatives of shape functions are

$$\begin{aligned} \frac{\partial N_j}{\partial \xi} &= \frac{1}{256} (1 + \eta\eta_j)[-10 + 9(\xi_j^2 + \eta_j^2)](-10\xi_j + 18\xi + 27\xi_j\xi^2 + 9\xi_j\eta^2) \\ &\quad + \frac{81}{256} \xi_j(1 + 9\eta\eta_j)(1 - \eta^2)(1 - \eta_j^2) \\ &\quad + \frac{81}{256} (1 + \eta\eta_j)(1 - \xi_j^2)(9\xi_j - 2\xi - 27\xi_j\xi^2) \end{aligned} \quad (7a)$$

$$\begin{aligned} \frac{\partial N_j}{\partial \eta} &= \frac{1}{256} (1 + \xi\xi_j)[-10 + 9(\xi^2 + \eta^2)](-10\eta_j + 18\eta + 27\eta_j\eta^2 + 9\eta_j\xi^2) \\ &\quad + \frac{81}{256} \eta_j(1 + 9\xi\xi_j)(1 - \xi^2)(1 - \xi_j^2) \\ &\quad + \frac{81}{256} (1 + \xi\xi_j)(1 - \eta_j^2)(9\eta_j - 2\eta - 27\eta_j\eta^2) \end{aligned} \quad (7b)$$

### THE CRACK TIP ELEMENT

In an 8-node quadratic isoparametric element, Henshell and Shaw [8] and Barsoum [9] found independently that the strain became singular at the corner node if the mid-side nodes were placed at the quarter points

<sup>8</sup>Henshell, R. D., and Shaw, K. G., "Crack Tip Finite Elements Are Unnecessary," International Journal for Numerical Methods in Engineering, Vol. 9, 1975.

<sup>9</sup>Barsoum, R. S., "On the Use of Isoparametric Finite Elements in Linear Fracture Mechanics," International Journal for Numerical Methods in Engineering, Vol. 10, 1976.

<sup>10</sup>Hussain, M. A., Lorensen, W. E., and Pflieg1, G., "The Quarter-Point Quadratic Isoparametric Element as a Singular Element for Crack Problems," NASA TM-X-3428, 1976, p. 419.

of the sides from the corner node. This singularity is achieved in a similar way for a 12-node isoparametric element by placing the two middle nodes at the 1/9 and 4/9 of the length of the sides from the common node of two sides.

For simplicity, let us consider the singularity along the side  $\eta = -1$  of Figure 1. In general, the cubic mapping functions are

$$x = a_0 + a_1\xi + a_2\xi^2 + a_3\xi^3 \quad (8)$$

$$u = b_0 + b_1\xi + b_2\xi^2 + b_3\xi^2 \quad (9)$$

For  $\xi = -1, -1/3, 1/3$  and  $1$ , the corresponding values of  $x$  and  $u$  are

$$x = 0, \alpha l, \beta l, l$$

$$u = u_1, u_2, u_3, u_4$$

The constants  $a$ 's and  $b$ 's in terms of these values of  $x$  and  $u$  are

$$\left. \begin{aligned} a_0 &= \frac{l}{16} (-1 + 9\alpha + 9\beta) & , & \quad a_1 = \frac{l}{16} (-1 - 27\alpha + 27\beta) \\ a_2 &= \frac{9l}{16} (1 - \alpha - \beta) & , & \quad a_3 = \frac{9l}{16} (1 + 3\alpha - 3\beta) \end{aligned} \right\} (10)$$

$$b_0 = \frac{1}{16} (-u_1 + 9u_2 + 9u_3 - u_4) \quad , \quad b_1 = \frac{1}{16} (u_1 - 27u_2 + 27u_3 - u_4) \quad (11)$$

$$b_2 = \frac{9}{16} (u_1 - u_2 - u_3 + u_4) \quad , \quad b_3 = \frac{9}{16} (-u_1 + 3u_2 - 3u_3 + u_4)$$

To have singular strain at  $x = 0$  ( $\xi = -1$ ), the reduced Jacobian,  $\frac{dx}{d\xi}$ , must vanish at  $\xi = -1$ . From (8) we have

$$\frac{dx}{d\xi} = a_1 + 2a_2\xi + 3a_3\xi^2 \quad (12)$$

For  $\xi = -1$ ,  $\frac{dx}{d\xi} = 0$  leads to the equation

$$\beta = 2\alpha + \frac{2}{9} \quad (13)$$

In order to have the inverse square root singularity for  $\frac{du}{dx}$ ,

$$\frac{du}{dx} = \frac{du}{d\xi} \frac{d\xi}{dx} = (b_1 + 2b_2\xi + 3b_3\xi^2) / \frac{dx}{d\xi}$$

$x$  must be a quadratic function of  $\xi$  so that the inverse gives  $\xi$  as a function of  $x^{1/2}$ . This leads to  $a_3 = 0$  or

$$1 + 3\alpha - 3\beta = 0 \quad (14)$$

The solution of (13) and (14) gives

$$\alpha = 1/9 \quad \text{and} \quad \beta = 4/9 \quad (15)$$

Equations (8) and (9) become

$$x = \frac{\ell}{4} (1 + \xi)^2 \quad \text{or} \quad \xi = -1 + 2\sqrt{\frac{x}{\ell}} \quad (16)$$

$$u = u_1 + \frac{1}{2} (-11u_1 + 18u_2 - 9u_3 + 2u_4) \sqrt{\frac{x}{\ell}} + \frac{9}{2} (2u_1 - 5u_2 + 4u_3 - u_4) \frac{x}{\ell} + \frac{9}{2} (-u_1 + 3u_2 - 3u_3 + u_4) \left(\frac{x}{\ell}\right)^{3/2} \quad (17)$$

From (17) it is clear  $\frac{du}{dx}$  has singularity of the order  $\frac{1}{\sqrt{x}}$  at  $x = 0$ .

The inverse square root singularity at  $x = 0$  along any other ray emanating from node 1 can be achieved by degenerating the quadrilateral element into a triangular element with the side 10, 11, 12, 1 collapsed to a point at the crack tip and placing grid points 2, 9 at  $\ell/9$  and 3, 8 at  $4\ell/9$  from the tip (Figure 2), where  $\ell$  is the length of the sides corresponding to  $\eta = \pm 1$ . The Cartesian coordinates of nodal points are shown in Figure 2. Using (3),

$$\left. \begin{aligned} x &= \frac{\ell}{8} (1 + \xi)^2 f(\eta, \alpha, \beta) \\ y &= \frac{\ell}{8} (1 + \xi)^2 f'(\eta, \alpha, \beta) \end{aligned} \right\} \quad (18)$$

where  $f$  and  $f'$  are abbreviations

$$f(\eta, \alpha, \beta) = (1 - \eta)\cos\beta + (1 + \eta)\cos\alpha$$

$$f'(\eta, \alpha, \beta) = (1 - \eta)\sin\beta + (1 + \eta)\sin\alpha$$

The Jacobian matrix is given by

$$[J] = \begin{bmatrix} \frac{\partial x}{\partial \xi} & \frac{\partial y}{\partial \xi} \\ \frac{\partial x}{\partial \eta} & \frac{\partial y}{\partial \eta} \end{bmatrix} = \begin{bmatrix} \frac{\ell}{4} (1 + \xi) f(\eta, \alpha, \beta) & \frac{\ell}{4} (1 + \xi) f'(\eta, \alpha, \beta) \\ \frac{\ell}{8} (1 + \xi)^2 (\cos\alpha - \cos\beta) & \frac{\ell}{8} (1 + \xi)^2 (\sin\alpha - \sin\beta) \end{bmatrix}$$

and the determinant

$$|J| = \frac{\ell^2}{16} (1 + \xi)^3 \sin(\alpha - \beta) \quad (19)$$

This shows the strain is singular at  $x = 0$  ( $\xi = -1$ ) along any ray from  $x = 0$  since  $|J| = 0$  at  $\xi = -1$  for all  $\eta$ .

For the inverse functions, we have

$$[J]^{-1} = \begin{bmatrix} \frac{\partial \xi}{\partial x} & \frac{\partial \eta}{\partial x} \\ \frac{\partial \xi}{\partial y} & \frac{\partial \eta}{\partial y} \end{bmatrix} = \begin{bmatrix} \frac{2(\sin\alpha - \sin\beta)}{\ell(1 + \xi)\sin(\alpha - \beta)} & \frac{-2(\cos\alpha - \cos\beta)}{\ell(1 + \xi)\sin(\alpha - \beta)} \\ \frac{-4f'(\eta, \alpha, \beta)}{\ell(1 + \xi)^2 \sin(\alpha - \beta)} & \frac{4f(\eta, \alpha, \beta)}{\ell(1 + \xi)^2 \sin(\alpha - \beta)} \end{bmatrix} \quad (20)$$

In terms of polar coordinates  $(r, \theta)$  we have from (18)

$$\left. \begin{aligned} 1 + \xi &= 2\sqrt{R} \quad , \quad R = (r/\ell)\cos(\theta - \frac{\alpha+\beta}{2})/\cos(\frac{\alpha-\beta}{2}) \\ \eta &= \tan(\theta - \frac{\alpha+\beta}{2})/\tan(\frac{\alpha-\beta}{2}) \end{aligned} \right\} \quad (21)$$



The displacements components  $u, v$  at a point  $(\xi, \eta)$  of the triangular element of Figure 2 are

$$\left. \begin{aligned} u &= \sum_{i=1}^{12} N_i(\xi, \eta) u_i = A_0(\eta, u_i) + A_1(\eta, u_i)(1 + \xi) \\ &\quad + A_2(\eta, u_i)(1 + \xi)^2 + A_3(\eta, u_i)(1 + \xi)^3 \\ v &= \sum_{i=1}^{12} N_i(\xi, \eta) v_i = A_0(\eta, v_i) + A_1(\eta, v_i)(1 + \xi) \\ &\quad + A_2(\eta, v_i)(1 + \xi)^2 + A_3(\eta, v_i)(1 + \xi)^3 \end{aligned} \right\} (22)$$

where

$$\begin{aligned} A_0(\eta, u_i) &= \{2(-1 + 9\eta^2)[(1 - \eta)u_1 + (1 + \eta)u_{10}] \\ &\quad + 18(1 - \eta^2)[(1 + 3\eta)u_{11} + (1 - 3\eta)u_{12}]\}/32 \end{aligned} \quad (23)$$

The displacement derivatives are

$$\begin{aligned} \frac{\partial u}{\partial x} &= \frac{\partial u}{\partial \xi} \frac{\partial \xi}{\partial x} + \frac{\partial u}{\partial \eta} \frac{\partial \eta}{\partial x} = \frac{1}{(1 + \xi)^2} \frac{-4f'(\eta, \alpha, \beta)}{l \sin(\alpha - \beta)} \frac{\partial A_0}{\partial \eta} \\ &+ \frac{1}{(1 + \xi)} \frac{2}{l \sin(\alpha - \beta)} \{(\sin \alpha - \sin \beta)A_1 - 2f'(\eta, \alpha, \beta) \frac{\partial A_1}{\partial \eta}\} + \dots \end{aligned} \quad (24)$$

$$\begin{aligned} \frac{\partial u}{\partial y} &= \frac{\partial u}{\partial \xi} \frac{\partial \xi}{\partial y} + \frac{\partial u}{\partial \eta} \frac{\partial \eta}{\partial y} = \frac{1}{(1 + \xi)^2} \frac{4f(\eta, \alpha, \beta)}{l \sin(\alpha - \beta)} \frac{\partial A_0}{\partial \eta} \\ &\frac{1}{(1 + \xi)} \frac{2}{l \sin(\alpha - \beta)} \{-(\cos \alpha - \cos \beta)A_1 + 2f(\eta, \alpha, \beta) \frac{\partial A_1}{\partial \eta}\} + \dots \end{aligned} \quad (25)$$

where

$$\begin{aligned} \frac{\partial A_0(\eta, u_i)}{\partial \eta} &= \{(2 + 36\eta - 54\eta^2)u_1 - (2 - 36\eta - 54\eta^2)u_{10} \\ &\quad + 18(3 - 2\eta - 9\eta^2)u_{11} - 18(3 + 2\eta - 9\eta^2)u_{12}\}/32 \end{aligned} \quad (26)$$

Similar expressions for  $\partial v/\partial x$  and  $\partial v/\partial y$  can be obtained by replacing  $u_i$  with  $v_i$ .

It can be seen that the strain field is singular at  $r = 0$ . The order of singularity is  $(1/r)$ . The leading term vanishes together with  $\partial A_0/\partial \eta$  for all  $\eta$  if

$$u_1 = u_{10} = u_{11} = u_{12} \quad , \quad v_1 = v_{10} = v_{11} = v_{12} \quad (27)$$

In this case, the order of singularity becomes  $(1/\sqrt{r})$ . This is analogous to the constraints given in [12] for quadratic, isoparametric elements. Hence we have two types of strain singularity at our disposition. If nodes 1, 10, 11, 12, which are collapsed into one point at the crack tip (Fig. 2), are tied together during deformation, the elastic singularity is obtained. If these nodes are allowed to slide with respect to each other, then the strain singularity is of the order of  $(1/r)$ , the perfect plastic singularity.

Using the multiple constraint conditions, equations (27), the displacement components at  $(\xi, \eta)$  relative to the tip may be written in the form

$$u = \frac{1}{16} \sqrt{R} [36F_1(\eta, u_i) + F_3(\eta, u_i) + 36\{F_2(\eta, u_i) - F_1(\eta, u_i)\} \sqrt{R} - 36F_2(\eta, u_i)R] \quad (28)$$

$$v = \frac{1}{16} \sqrt{R} [36F_1(\eta, v_i) + F_3(\eta, v_i) + 36\{F_2(\eta, v_i) - F_1(\eta, v_i)\} \sqrt{R} - 36F_2(\eta, v_i)R] \quad (29)$$

where

$$\left. \begin{aligned}
 F_1(\eta, u_i) &= (1 - \eta)(2u_2 - u_3) + (1 + \eta)(2u_9 - u_8) \\
 F_2(\eta, u_i) &= (1 - \eta)(-3u_2 + 3u_3 - u_4) + (1 + \eta)(-3u_9 + 3u_8 - u_7) \\
 F_3(\eta, u_i) &= 9(1 - \eta^2)[(1 - 3\eta)u_5 + (1 + 3\eta)u_6] \\
 &\quad - (1 - 9\eta^2)[(1 - \eta)u_4 + (1 + \eta)u_7]
 \end{aligned} \right\} (30)$$

and  $F_1(\eta, v_i)$  etc. are obtained by replacing  $u_i$  with  $v_i$ .

#### DETERMINATION OF STRESS INTENSITY FACTORS

The collapsed, triangular elements around the crack tip have the correct elastic singularity at the tip if all nodes at the tip are tied together during deformation. Only one set of displacement functions is used for regular quadrilateral elements and the collapsed triangular elements. Hence the continuity of displacement components is insured throughout the region. The nodal displacements obtained from the finite element method using higher order polynomials for the displacement field should be quite accurate. In this section, we will briefly discuss various techniques to estimate the stress intensity factors from the nodal displacements thus obtained. The discussion is limited to the use of nodal displacements. Other techniques, such as J-integral, the strain energy release rate etc. are not included.

The well known classical near crack tip displacements are given by [13]

<sup>13</sup>Williams, M. L., "On the Stress Distribution at the Base of a Stationary Crack," Journal of Applied Mechanics, Vol. 24, 1957.

$$2Gu(\theta) = \sum_{n=1,2,\dots} \{(-1)^{n-1} r^{n-1/2} [d_{2n-1} D_{u1}(n,\theta) + a_{2n-1} A_{u1}(n,\theta)] + (-1)^n r^n [d_{2n} D_{u2}(n,\theta) + a_{2n} A_{u2}(n,\theta)]\} \quad (31)$$

$$2Gv(\theta) = \sum_{n=1,2,\dots} \{(-1)^{n-1} r^{n-1/2} [d_{2n-1} D_{v1}(n,\theta) + a_{2n-1} A_{v1}(n,\theta)] + (-1)^n r^n [d_{2n} D_{v2}(n,\theta) + a_{2n} A_{v2}(n,\theta)]\} \quad (32)$$

where

$$\left. \begin{aligned} D_{u1}(n,\theta) &= (n - 1/2)\cos(n - \frac{5}{2})\theta - (\kappa + n - \frac{3}{2})\cos(n - \frac{1}{2})\theta \\ D_{u2}(n,\theta) &= n\cos(n - 2)\theta - (\kappa + n + 1)\cos n\theta \\ A_{u1}(n,\theta) &= (n - 1/2)\sin(n - \frac{5}{2})\theta - (\kappa + n + 1/2)\sin(n - 1/2)\theta \\ A_{u2}(n,\theta) &= n\sin(n - 2)\theta - (\kappa + n - 1)\sin n\theta \\ D_{v1}(n,\theta) &= -(n - 1/2)\sin(n - \frac{5}{2})\theta - (\kappa - n + \frac{3}{2})\sin(n - \frac{1}{2})\theta \\ D_{v2}(n,\theta) &= -n\sin(n - 2)\theta - (\kappa - n - 1)\sin n\theta \\ A_{v1}(n,\theta) &= (n - \frac{1}{2})\cos(n - \frac{5}{2})\theta + (\kappa - n - 1/2)\cos(n - 1/2)\theta \\ A_{v2}(n,\theta) &= n\cos(n - 2)\theta + (\kappa - n + 1)\cos n\theta \end{aligned} \right\} \quad (33)$$

in which

$$\kappa = \begin{cases} (3 - \nu)/(1 + \nu) & \text{for plane stress} \\ 3 - 4\nu & \text{for plane strain} \end{cases} \quad (34)$$

The coefficients d's and a's are to be determined from the boundary conditions of a problem. The stress intensity factors  $K_1$  and  $K_2$  are related to  $d_1$  and  $a_1$  by

$$K_1 = -d_1\sqrt{2\pi} \quad , \quad K_2 = -a_1\sqrt{2\pi} \quad (35)$$

In (31) and (32),  $u$  and  $v$  are displacement components referring to the local Cartesian coordinates with crack tip as the origin and the crack on the negative  $x$ -axis. A simple transformation can be used to change the nodal displacements in global coordinates, obtained from the finite element method, to displacements in local coordinates. For simplicity, we will assume the local coordinates and the global coordinates are the same.

#### 1. One Term Expansion:

If we retain only the  $\sqrt{r}$  term and drop all higher order terms in the right hand sides of (31) and (32), we shall obtain a set of  $d_1$  and  $a_1$  by substituting the displacement components of a nodal point into the left hand sides of (31) and (32). Numerical results thus obtained for  $K_1$  and  $K_2$  vary considerably depending on the locations of nodal points and the values of displacement components used. From (28) and (29), the displacement components of a collapsed triangular element are functions of  $r^{1/2}$ ,  $r$  and  $r^{3/2}$ . If  $u^*$  and  $v^*$  designate the leading portion of displacements ( $r^{1/2}$  term only) in (28) and (29), we have specifically

$$\left. \begin{aligned} u^*(\eta = -1) &= \frac{1}{2} (r/\ell)^{1/2} (18u_2 - 9u_3 + 2u_4) \\ u^*(\eta = 1) &= \frac{1}{2} (r/\ell)^{1/2} (18u_9 - 9u_8 + 2u_7) \end{aligned} \right\} \quad (36)$$

and similar expressions for  $v^*$  (replacing  $u$  by  $v$ ). The stress intensity factors obtained from (35) with  $d_1$  and  $a_1$  computed from (31) and (32) using  $u^*$ ,  $v^*$  on the left hand sides and using only the  $\sqrt{r}$  term in the right hand sides, are independent of  $r$ . The use of the leading portion of displacements  $u^*$  or  $v^*$  on the left hand sides of (31) and (32) is suggested by Tracey [14] and discussed by Barsoum [15]. For a mode I (or mode II) crack, all  $a$ 's (or  $d$ 's) of (31) and (32) vanish. The stress intensity factor  $K_1$  (or  $K_2$ ) can be obtained by either (31) or (32).

## 2. Two-Term Expansion:

In (31) and (32), if  $r^{1/2}$  and  $r$  terms are considered, we have four unknown constants  $d_1$ ,  $a_1$ ,  $d_2$ ,  $a_2$  to be determined. Four displacement components of any two nodal points should suffice to compute  $K_1$  and  $K_2$ . In practice, we use either the pair of nodes (2,9) or (3,8) of Figure 2. Two nodes of different  $r$  such as (2,3) or (8,9) usually give poorer results. On the left hand side of (28) and (29), we may use actual nodal displacements  $(u_2, v_2)$ ,  $(u_9, v_9)$  or we may use  $(u_2^{**}, v_2^{**})$  and  $(u_9^{**}, v_9^{**})$  where  $u_2^{**}$  is the part of  $u_2$  corresponding to  $r^{1/2}$  and  $r$  terms in (28). For  $\eta = \pm 1$

<sup>14</sup>Tracey, D. M., "Discussion of 'On the Use of Isoparametric Finite Elements in Linear Fracture Mechanics' by R. S. Barsoum," Int. Journal for Numerical Methods in Engineering, Vol. 11, 1977.

<sup>15</sup>Barsoum, R. S., "Author's Reply to the Discussion by Tracey," Int. Journal for Numerical Methods in Engineering, Vol. 11, 1977.

$$\left. \begin{aligned}
 u^{**}(\eta = -1) &= \frac{1}{2} (r/\ell)^{1/2} (18u_2 - 9u_3 + 2u_4) - \frac{9}{2} (r/\ell) (5u_2 - 4u_3 + u_4) \\
 u^{**}(\eta = 1) &= \frac{1}{2} (r/\ell)^{1/2} (18u_9 - 9u_8 + 2u_7) - \frac{9}{2} (r/\ell) (5u_9 - 4u_8 + u_7)
 \end{aligned} \right\} \quad (37)$$

For a mode I crack, both  $a_1$  and  $a_2$  vanish. Only two displacement components of a node are needed to determine  $d_1$  and  $d_2$ . Any of the following pairs may be used for this purpose:  $(u_2, v_2)$ ,  $(u_3, v_3)$ ,  $(u_9, v_9)$ ,  $(u_8, v_8)$ .

### 3. Four Term Expansion:

If we take  $r^{1/2}$  up to  $r^2$  terms in (31) and (32), the eight constants  $d_i$  and  $a_i$ ,  $i = 1, 2, 3, 4$  are to be determined from displacement components of four nodal points. We may take two mid-nodes ( $\ell/9$  and  $4\ell/9$  from the tip) of the two sides of a collapsed triangular element as the four nodal points, or we may take four consecutive nodes of the same radius from the tip ( $r = \ell/9$  or  $r = 4\ell/9$ ). For the three collapsed triangular elements around a mode I crack shown in Figure 5(a), displacement components are taken from one of the following three groups: (i) nodes 11, 12, 13, 14; (ii) nodes 15, 16, 17, 18; (iii) nodes 11, 12, 15, 16 of the element (1), nodes 12, 13, 16, 17 of the element (2) and nodes 13, 14, 17, 18 of the element (3).

### 4. Collocation Method:

Let  $u_s, v_s$  be displacements from the asymptotic expansions (31) and (32) and let  $u_e$  and  $v_e$  be displacements from finite elements given by (28) and (29). For an arbitrarily fixed  $r$ , we define

$$\epsilon = \sum_{i=1}^N \{ [u_s(\theta_i) - u_e(\theta_i)]^2 + [v_s(\theta_i) - v_e(\theta_i)]^2 \} \quad (38)$$

The unknown coefficients d's and a's in (31) and (32) are the set which minimizes  $\epsilon$ . In other words, d's and a's are solutions of

$$\left. \begin{array}{l} \frac{\partial \epsilon}{\partial d_j} = 0 \\ \frac{\partial \epsilon}{\partial a_j} = 0 \end{array} \right\} j = 1, 2, \dots, n \leq \frac{N}{2} \quad (39)$$

where  $n = 2p$ ,  $p$  is the highest exponent of  $r$  in the asymptotic expansion.

#### NASTRAN IMPLEMENTATION

The NASTRAN implementation of the 12-node quadrilateral follows that of the 8-node quadrilateral as described in [10]. The dummy users element facility of NASTRAN is used. This requires coding routines to calculate element stiffness matrices and stress recovery computations. Modifications to existing NASTRAN source codes are made to provide proper output formats for the element. Three-point Gaussian quadrature is normally used to calculate each partial integration of the double integral (4). As an option a four-point Gaussian quadrature may be used instead. All stiffness computations are performed in double precision while stress recovery is performed in single precision. Element stiffness matrix computation requires 10 seconds/element on an IBM 360/44. Stress intensity factors are calculated from nodal displacements by various techniques. Equations

<sup>10</sup>Hussain, M. A., Lorensen, W. E., and Pflagl, G., "The Quarter-Point Quadratic Isoparametric Element As a Singular Element for Crack Problems," NASA TM-X-3428, 1976, p. 419.



(40) are finally adopted to compute stress intensity factors for mode I, mode II and mixed mode cracks.

### NUMERICAL RESULTS

Computer program APES [16] utilizes the same 12-node quadrilateral isoparametric elements shown in Figure 1. The high order element greatly reduces the total number of elements as well as nodal points needed to model either elasticity or fracture problems. The program has been designed primarily for user convenience. There are many convenient features such as the automatic generation of middle nodes of a side which is a straight line, and the automatic computation of nodal force for a given distributed and/or concentrated tractions.

However, APES requires the use of special crack tip elements for fracture problems. There are two different types of crack tip elements used in APES. One is a small circular core element which completely encloses a crack tip and which reproduces the singular nature of the strains there. The other consists of several "enriched" 12-node elements around a crack tip all having a corner node corresponding to the tip. In an enriched element, the displacement assumption is augmented by the leading terms of the singular near field solution (an extension of the work of Benzley and Beisinger [7]). Both models lead to about the same high degree of accuracy in stress intensity factors  $K_1$  and  $K_2$ .

---

<sup>7</sup>Benzley, S. E. and Beisinger, A. E., "Chiles - A Finite Element Computer Program That Calculates the Intensities of Linear Elastic Singularities," Sandia Laboratories, Technical Report SLA-73-0894, 1973.

<sup>16</sup>Gifford, L. N., "Apes - Second Generation Two-Dimensional Fracture Mechanics and Stress Analysis by Finite Elements," Naval Ship Research and Development Center, Report 4799, December 1975.

In this report, we have used the collapsed triangular elements to eliminate the use of these special crack tip elements. The same displacement functions are used for quadrilateral elements and triangular elements, and there is no question regarding the continuity of displacement between the special crack tip elements and conventional QUAD-12 elements. There is no need for the use of 8 x 8 Gaussian quadrature for numerical integration of element stiffness matrix as is required for the enriched QUAD-12 elements. From the numerical results, the collapsed triangular elements as singular crack tip elements will be assessed.

Three mode I crack problems and one mixed mode crack problem are chosen for numerical computation of stress intensity factors. The geometries and loads of mode I tension test specimens are given in Figure 3. The idealization of a half of the single edge crack is shown in Figure 4. Similar idealization is used also for a quadrant of a center crack or a double edge crack. Three collapsed triangular elements surrounding a mode I crack tip are shown in Figure 5(a). The same idealization is used for NASTRAN and APES (with collapsed triangular elements). For comparison, a circular core with 10-core nodes around the crack tip is also used in APES and is shown in Figure 5(b). Around a mixed mode crack tip, six collapsed triangular elements, shown in Figure 6(a), are used and the corresponding singular 'core' element surrounded by six QUAD-12 elements are shown in Figure 6(b). A 45° slant edge crack, in a rectangular panel under tension, is taken as an example of mixed mode cracks and is shown in Figure 7. The

sixteen-element idealization of the cracked panel is also shown in the same figure, and the six elements around the crack tip are enlarged and shown in Figure 6.

Our first goal in the numerical analysis is to find a simple and accurate way to estimate the stress intensity factor from nodal displacements obtained from the finite element method. For the purpose of comparison, stress intensity factors obtained from the finite element method are normalized by corresponding values which are considered as exact. Referring to Figure 3,  $K_I = 1.966$  [17] is taken as exact for the central crack and  $K_I = 2.00$  [18] for the double edge crack. For the single edge crack  $K_I = 3.728$  for  $a/b = 0.4$ ,  $H/b = 4$  and  $K_I = 5.009$  for  $a/b = 0.5$ ,  $H/b = 3$  (first  $F(a/b)$  on page 2.11 of [19]). Normalized stress intensity factors for the three mode I crack specimens are computed by APES, using singular 'core' element with 10-core nodes, Figure 5(b). Results are tabulated in Table 1 for  $h/r_0 = 6$  and  $r_0 = 0.01, 0.02$  and  $0.03$ . The overall results are better for  $r_0/a = 0.01$ . Here and in tables 1 through 8,  $r_0 = 0.01, 0.015, \dots$  should be understood as  $r_0/a = 0.01, 0.015, \dots$  since  $a = 1$  is used for all mode I crack examples.

---

<sup>17</sup>Isida, M., "Analysis of Stress Intensity Factors for the Tension of a Centrally Cracked Strip with Stiffened Edges," Engineering Fracture Mechanics, Vol. 5, 1973.

<sup>18</sup>Brown, W. F., and Srawley, J. E., "Plane Strain Crack Toughness Testing of High Strength Metallic Materials," ASTM STP-410, 1966.

<sup>19</sup>Tada, H., Paris, P., and Irwin, G., The Stress Analysis of Cracks Handbook, Del Research Corp., 1973.

TABLE 1. RATIOS OF  $K_I$  (APES) TO  $K_I$  (EXACT)

	$r_0 = 0.01$	$r_0 = 0.02$	$r_0 = 0.03$
Center crack (exact $K_I = 1.966$ )	0.996	0.976	0.969
Double edge crack (exact $K_I = 2.00$ )	1.001	0.993	0.989
Single edge crack (exact $K_I = 5.009$ )	0.974	0.964	0.966

Replacing the special core element and the regular 12-node, quadrilateral elements surrounding the core with collapsed triangular elements, we can use the APES program for general structures (no cracks) to obtain displacement components at all nodes. Stress intensity factors are then obtained from displacements at nodes close to the crack tip by various techniques mentioned previously. If only one term expansion is used, the ratios of  $K_I$  (Finite Element) to  $K_I$  (Exact) for the three tension test specimens are given in Tables 2-4. The use of  $v^*$  (leading term of  $v$ ) does not always give better results (e.g. Table 4). Using two term expansion, the same ratios are given in Tables 5-7. The results from two term expansion show little improvement. Similar results using four term expansion are tabulated in Table 8. The values in the last column of Table 8 are the linear average of three values of  $K_I$  obtained from three different elements. Careful study of results tabulated in Tables 2 through 8 reveals that one term expansion using  $v$  at node 14 or 18, Figure 5(a), with  $r_0 = 1\% - 2\%$  of the crack length is the simplest way to estimate  $K_I$  and  $K_I$  thus obtained is quite accurate. This technique is adopted in our NASTRAN to compute  $K_I$ .

TABLE 2.  $K_I$  (FINITE ELEMENT)/ $K_I$  (EXACT) BY ONE-TERM EXPANSION USING APES

WITH COLLAPSED TRIANGULAR ELEMENTS

Center Crack $a/b=0.4, H/b=4$ EXACT $K_I=1.966$	Based on $u(r, \theta)$ & $v(r, \theta)$		$u^*$ & $v^*$		Based on $u(r, \theta)$		Based on $v(r, \theta)$		$v^*(r, \theta)$	
	$r=r_0$	$r=4r_0$	$r_0$ or $4r_0$	$r=r_0$	$r=4r_0$	$r_0$ or $4r_0$	$r=r_0$	$r=4r_0$	$r=r_0$	$r=4r_0$
$r_0=0.010$	$\theta=0^\circ$	0.879	0.779	1.013	0.879	0.779	0.992	-	-	-
	60°	1.019	1.049	1.009	0.949	0.896	1.001	1.045	1.106	0.982
	120°	1.014	1.035	1.019	1.019	1.043	0.977	1.015	1.036	0.988
	180°	0.998	0.998	1.013	-	-	-	0.998	0.998	0.982
	AVERAGE	0.978	0.965	1.014	0.949	0.906	0.990	1.019	1.047	0.984
$r_0=0.015$	$\theta=0^\circ$	0.852	0.737	1.005	0.852	0.737	0.984	-	-	-
	60°	1.015	1.047	1.007	0.932	0.869	0.990	1.046	1.114	0.983
	120°	1.009	1.026	1.014	1.023	1.048	0.975	1.009	1.026	0.986
	180°	0.990	0.985	1.012	-	-	-	0.990	0.985	0.938
	AVERAGE	0.966	0.949	1.010	0.936	0.885	0.983	1.015	1.042	0.984
$r_0=0.020$	$\theta=0^\circ$	0.833	0.703	1.002	0.833	0.703	0.981	-	-	-
	60°	1.015	1.051	1.009	0.922	0.849	0.987	1.051	1.127	0.986
	120°	1.008	1.023	1.015	1.028	1.052	0.976	1.009	1.024	0.987
	180°	0.988	0.977	1.014	-	-	-	0.988	0.977	0.986
	AVERAGE	0.961	0.938	1.010	0.928	0.868	0.981	1.016	1.043	0.986
$r_0=0.025$	$\theta=0^\circ$	0.817	0.675	1.001	0.817	0.674	0.980	-	-	-
	60°	1.017	1.056	1.010	0.913	0.831	0.986	1.056	1.141	0.988
	120°	1.008	1.022	1.016	1.034	1.054	0.979	1.009	1.023	0.989
	180°	0.986	0.970	1.015	-	-	-	0.986	0.970	0.988
	AVERAGE	0.957	0.931	1.011	0.921	0.850	0.982	1.017	1.045	0.988

TABLE 3.  $K_I$  (FINITE ELEMENT)/ $K_I$  (EXACT) BY ONE-TERM EXPANSION USING APES

WITH COLLAPSED TRIANGULAR ELEMENTS

Double Edge Crack $a/b=0.4, H/b=4.0$ EXACT $K_I=2.00$	Based on $u(r, \theta)$ & $v(r, \theta)$		$u^*$ & $v^*$ $r_0$ or $4r_0$	Based on $u(r, \theta)$		$u^*(r, \theta)$ $r_0$ or $4r_0$	Based on $v(r, \theta)$		$v^*(r, \theta)$ $r_0$ or $4r_0$
	$r=r_0$	$r=4r_0$		$r=r_0$	$r=4r_0$		$r=r_0$	$r=4r_0$	
$r_0=0.010$	$\theta=0^\circ$	0.946	0.898	0.975	0.946	0.898	0.996	-	-
	$60^\circ$	1.009	1.028	0.970	0.971	0.946	1.000	1.023	0.989
	$120^\circ$	1.018	1.029	0.972	1.006	1.014	0.987	1.017	1.001
	$180^\circ$	1.005	1.003	0.966	-	-	-	1.005	0.996
	AVERAGE	0.994	0.989	0.971	0.974	0.953	0.994	1.015	1.030
$r_0=0.015$	$\theta=0^\circ$	0.930	0.875	0.967	0.930	0.875	0.988	-	-
	$60^\circ$	1.004	1.025	0.969	0.962	0.932	0.991	1.020	0.990
	$120^\circ$	1.010	1.017	0.970	1.005	1.014	0.983	1.010	0.997
	$180^\circ$	0.997	0.992	0.967	-	-	-	0.997	0.995
	AVERAGE	0.985	0.977	0.968	0.966	0.940	0.987	1.009	1.023
$r_0=0.020$	$\theta=0^\circ$	0.920	0.858	0.965	0.920	0.858	0.985	-	-
	$60^\circ$	1.005	1.028	0.970	0.957	0.923	0.988	1.023	0.993
	$120^\circ$	1.008	1.013	0.971	1.007	1.016	0.985	1.008	0.997
	$180^\circ$	0.995	0.986	0.969	-	-	-	0.995	0.997
	AVERAGE	0.982	0.971	0.969	0.961	0.933	0.986	1.009	1.022
$r_0=0.025$	$\theta=0^\circ$	0.912	0.844	0.963	0.912	0.844	0.984	-	-
	$60^\circ$	1.006	1.032	0.971	0.953	0.916	0.988	1.027	0.995
	$120^\circ$	1.007	1.011	0.972	1.010	1.017	0.989	1.007	0.998
	$180^\circ$	0.994	0.982	0.972	-	-	-	0.994	0.998
	AVERAGE	0.980	0.967	0.969	0.958	0.925	0.987	1.009	1.023

TABLE 4.  $K_I$  (FINITE ELEMENT)/ $K_I$  (EXACT) BY ONE-TERM EXPANSION USING APES  
WITH COLLAPSED TRIANGULAR ELEMENTS

Single Edge Crack $a/b=0.5, H/b=3.0$ EXACT $K_I=5.009$	Based on $u(r, \theta)$ & $v(r, \theta)$		$u^* & v^*$ $r_0$ or $4r_0$	Based on $u(r, \theta)$		$u^*(r, \theta)$ $r_0$ or $4r_0$	Based on $v(r, \theta)$		$v^*(r, \theta)$ $r_0$ or $4r_0$
	$r=r_0$	$r=4r_0$		$r=r_0$	$r=4r_0$		$r=r_0$	$r=4r_0$	
$r_0=0.010$	$\theta=0^\circ$	0.920	0.898	0.939	0.920	0.939	-	-	-
	$60^\circ$	0.970	0.973	0.959	0.951	0.954	0.977	0.982	0.960
	$120^\circ$	0.980	0.992	0.968	0.951	0.934	0.979	0.991	0.967
	$180^\circ$	0.972	0.983	0.958	-	-	0.972	0.983	0.958
	AVERAGE	0.960	0.961	0.956	0.941	0.942	0.976	0.985	0.962
$r_0=0.015$	$\theta=0^\circ$	0.927	0.899	0.948	0.927	0.948	-	-	-
	$60^\circ$	0.967	0.966	0.960	0.955	0.955	0.972	0.970	0.962
	$120^\circ$	0.974	0.986	0.965	0.962	0.942	0.974	0.986	0.964
	$180^\circ$	0.969	0.983	0.958	-	-	0.969	0.983	0.958
	AVERAGE	0.959	0.958	0.958	0.954	0.948	0.972	0.980	0.961
$r_0=0.020$	$\theta=0^\circ$	0.934	0.898	0.959	0.934	0.959	-	-	-
	$60^\circ$	0.968	0.895	0.963	0.961	0.960	0.971	0.963	0.964
	$120^\circ$	0.974	0.986	0.966	0.975	0.952	0.974	0.987	0.965
	$180^\circ$	0.970	0.987	0.960	-	-	0.970	0.987	0.960
	AVERAGE	0.962	0.959	0.962	0.956	0.957	0.972	0.979	0.963
$r_0=0.025$	$\theta=0^\circ$	0.940	0.896	0.968	0.940	0.968	-	-	-
	$60^\circ$	0.970	0.961	0.966	0.966	0.967	0.971	0.957	0.966
	$120^\circ$	0.975	0.988	0.967	0.986	0.960	0.976	0.990	0.967
	$180^\circ$	0.972	0.992	0.962	-	-	0.972	0.992	0.962
	AVERAGE	0.964	0.959	0.966	0.964	0.965	0.973	0.980	0.965

TABLE 5.  $K_I$  (FINITE ELEMENT)/ $K_I$  (EXACT) BY TWO-TERM EXPANSION USING APES  
WITH COLLAPSED TRIANGULAR ELEMENTS

Center Crack $a/b=0.4, H/b=4.0$ EXACT $K_I=1.966$	BASED ON DISPLACEMENT COMPONENTS OF TWO ADJACENT NODES OF A TRIANGULAR ELEMENT											
	$u(r,\theta) \text{ \& \ } v(r,\theta)$		$u^*(r,\theta) \text{ \& \ } v^*(r,\theta)$		$u^{**}(r,\theta) \text{ \& \ } v^{**}(r,\theta)$		$u(r,\theta)$		$v(r,\theta)$			
	$r=r_0$	$r=4r_0$	$r=r_0$ or $r=4r_0$	$r=r_0$	$r=4r_0$	$r=r_0$	$r=4r_0$	$r=r_0$	$r=4r_0$	$r=r_0$	$r=4r_0$	$r=r_0$
ELEM. ① ② ③ AVERAGE $r_0=0.010$	1.002	1.022	0.984	1.001	1.018	0.994	0.972	-	-	0.998	-	-
	1.004	1.015	0.991	1.004	1.017	0.983	0.967	0.998	0.998	0.998	0.998	0.996
	1.063	1.087	1.149	1.008	0.868	0.988	0.964	0.998	0.998	0.998	0.998	0.998
	1.023	1.042	1.041	1.004	0.968	0.988	0.968	0.998	0.998	0.998	0.998	0.997
ELEM. ① ② ③ AVERAGE $r_0=0.015$	0.995	1.016	0.983	0.991	0.999	0.984	0.956	0.984	0.984	0.989	-	-
	0.996	1.005	0.988	0.995	1.003	0.976	0.956	0.976	0.976	0.990	0.979	0.979
	1.032	1.046	1.027	1.005	0.937	0.980	0.949	0.980	0.980	0.990	0.990	0.985
	1.008	1.022	1.015	0.997	0.979	0.980	0.954	0.980	0.980	0.990	0.990	0.982
ELEM. ① ② ③ AVERAGE $r_0=0.020$	0.994	1.018	0.984	0.987	0.990	0.979	0.944	0.979	0.979	0.986	-	-
	0.993	1.001	0.988	0.992	0.995	0.974	0.948	0.974	0.974	0.986	0.968	0.968
	1.013	1.025	1.040	0.994	0.948	0.975	0.935	0.975	0.975	0.988	0.977	0.977
	1.000	1.015	1.004	0.991	0.978	0.976	0.942	0.976	0.976	0.987	0.987	0.973
ELEM. ① ② ③ AVERAGE $r_0=0.025$	0.994	1.021	0.985	0.985	0.984	0.975	0.932	0.975	0.975	0.984	-	-
	0.992	0.999	0.989	0.989	0.990	0.972	0.939	0.972	0.972	0.984	0.959	0.959
	1.000	1.013	1.023	0.981	0.939	0.972	0.923	0.972	0.972	0.986	0.970	0.970
	0.995	1.011	0.999	0.985	0.971	0.973	0.931	0.973	0.973	0.985	0.985	0.964



TABLE 6.  $K_I$  (FINITE ELEMENT)/ $K_I$  (EXACT) BY TWO-TERM EXPANSION USING APES  
WITH COLLAPSED TRIANGULAR ELEMENTS

Double Edge Crack $a/b=0.4$ , $H/b=4.0$ EXACT $K_I=2.00$	BASED ON DISPLACEMENT COMPONENTS OF TWO ADJACENT NODES OF A TRIANGULAR ELEMENT											
	$u(r,\theta)$ & $v(r,\theta)$		$u^*(r,\theta)$ & $v^*(r,\theta)$		$u^{**}(r,\theta)$ & $v^{**}(r,\theta)$		$u(r,\theta)$		$v(r,\theta)$			
	$r=r_0$	$r=4r_0$	$r=r_0$	$r=4r_0$	$r=r_0$	$r=4r_0$	$r=r_0$	$r=4r_0$	$r=r_0$	$r=4r_0$	$r=r_0$	$r=4r_0$
$r_0=0.10$	ELEM. ①	1.003	1.018	0.991	1.002	1.012	0.988	0.977	0.988	0.977	0.988	0.977
	②	1.007	1.015	0.999	1.006	1.014	0.988	0.979	0.988	0.979	0.988	0.979
	③	1.058	1.096	1.088	1.023	0.959	0.990	0.974	0.990	0.974	0.990	0.974
	AVERAGE	1.023	1.043	1.026	1.010	0.995	0.989	0.977	0.989	0.977	0.989	0.977
$r_0=0.015$	ELEM. ①	0.997	1.013	0.989	0.993	0.997	0.982	0.970	0.982	0.970	0.982	0.970
	②	0.999	1.006	0.995	0.998	1.001	0.983	0.972	0.983	0.972	0.983	0.972
	③	1.031	1.061	1.026	1.018	1.011	0.983	0.966	0.983	0.966	0.983	0.966
	AVERAGE	1.009	1.026	1.003	1.003	1.003	0.982	0.969	0.982	0.969	0.982	0.969
$r_0=0.020$	ELEM. ①	0.996	1.014	0.991	0.990	0.990	0.980	0.966	0.980	0.966	0.980	0.966
	②	0.997	1.003	0.995	0.995	0.996	0.981	0.968	0.981	0.968	0.981	0.968
	③	1.015	1.045	1.007	1.005	1.003	0.980	0.960	0.980	0.960	0.980	0.960
	AVERAGE	1.003	1.021	0.998	0.997	0.996	0.981	0.965	0.981	0.965	0.981	0.965
$r_0=0.025$	ELEM. ①	0.997	1.017	0.992	0.989	0.986	0.980	0.962	0.980	0.962	0.980	0.962
	②	0.997	1.003	0.996	0.994	0.993	0.981	0.965	0.981	0.965	0.981	0.965
	③	1.005	1.038	1.006	0.988	0.969	0.978	0.954	0.978	0.954	0.978	0.954
	AVERAGE	1.000	1.019	0.998	0.990	0.983	0.980	0.960	0.980	0.960	0.980	0.960

TABLE 7.  $K_I$  (FINITE ELEMENT)/ $K_I$  (EXACT) BY TWO-TERM EXPANSION USING APES  
WITH COLLAPSED TRIANGULAR ELEMENTS

Single Edge Crack $a/b=0.5$ , $H/b=3$ EXACT $K_I=5.009$	BASED ON DISPLACEMENT COMPONENTS OF TWO ADJACENT NODES OF A TRIANGULAR ELEMENT											
	$u(r,\theta) \text{ \& \ } v(r,\theta)$		$u^*(r,\theta) \text{ \& \ } v^*(r,\theta)$		$u^{**}(r,\theta) \text{ \& \ } v^{**}(r,\theta)$		$u(r,\theta)$		$v(r,\theta)$			
	$r=r_0$	$r=4r_0$	$r=r_0$ or $r=4r_0$	$r=r_0$	$r=4r_0$	$r=r_0$	$r=4r_0$	$r=r_0$	$r=4r_0$	$r=r_0$	$r=4r_0$	$r=r_0$
$r_0=0.010$	ELEM. ①	0.961	0.960	0.954	0.966	0.977	0.972	0.982	-	-	-	-
	②	0.974	0.978	0.966	0.976	0.986	0.951	0.961	0.980	0.980	0.996	0.996
	③	1.052	1.055	1.112	1.020	0.928	0.960	0.973	0.972	0.972	0.983	0.983
AVERAGE	0.996	0.997	1.011	0.987	0.963	0.961	0.976	0.972	0.976	0.976	0.989	0.989
$r_0=0.015$	ELEM. ①	0.960	0.950	0.958	0.965	0.971	0.974	0.993	-	-	-	-
	②	0.969	0.970	0.964	0.972	0.979	0.959	0.976	0.975	0.975	0.995	0.995
	③	1.023	1.015	1.051	1.013	0.976	0.964	0.990	0.969	0.969	0.983	0.983
AVERAGE	0.984	0.978	0.991	0.983	0.976	0.966	0.987	0.987	0.972	0.972	0.989	0.989
$r_0=0.020$	ELEM. ①	0.961	0.944	0.963	0.968	0.974	0.979	1.007	-	-	-	-
	②	0.969	0.967	0.966	0.972	0.978	0.968	0.992	0.976	0.976	1.001	1.001
	③	1.008	0.995	1.032	1.002	0.973	0.971	1.007	0.970	0.970	0.987	0.987
AVERAGE	0.979	0.969	0.987	0.981	0.975	0.972	1.002	1.002	0.973	0.973	0.994	0.994
$r_0=0.025$	ELEM. ①	0.963	0.939	0.966	0.973	0.979	0.984	1.022	-	-	-	-
	②	0.970	0.966	0.968	0.973	0.978	0.976	1.006	0.978	0.978	1.008	1.008
	③	0.996	0.981	1.028	0.988	0.948	0.977	1.023	0.972	0.972	0.992	0.992
AVERAGE	0.976	0.962	0.987	0.978	0.968	0.979	0.979	1.017	0.975	0.975	1.000	1.000

TABLE 8.  $K_I$  (FINITE ELEMENT) BY FOUR-TERM EXPANSION USING APES  
 $K_I$  (EXACT)  
 WITH COLLAPSED TRIANGULAR ELEMENTS

	$r_0$	Based on U and V of Four Nodes of		
		Same $r$ , $r=r_0$	Same $r$ , $r=4r_0$	Same Element
Center Crack $a/b=0.4$ , $H/b=4.0$ EXACT $K_I=1.966$	0.010	1.005	1.018	0.969
	0.015	0.996	1.005	0.973
	0.020	0.993	0.999	0.978
	0.025	0.991	0.996	0.982
Double Edge Crack $a/b=0.4$ , $H/b=4.0$ EXACT $K_I=2.00$	0.010	1.013	1.022	0.988
	0.015	1.004	1.009	0.989
	0.020	1.001	1.004	0.993
	0.025	0.999	1.002	0.996
Single Edge Crack $a/b=0.5$ , $H/b=3.0$ EXACT $K_I=5.009$	0.010	0.979	0.985	0.945
	0.015	0.973	0.976	0.951
	0.020	0.972	0.973	0.958
	0.025	0.973	0.972	0.964

The collocation method requires the computation of displacements along  $r=r_0$  at points between nodes. For the single edge tension specimen with  $a/b=0.5$ ,  $H/b=3.0$ , the numerical results obtained from the collocation method are given in Table 9. It can be seen that values of  $K_I$  remain nearly a constant no matter how many terms or how many mid-points are taken. Because of more computations involved and since as good or even better results can be obtained by other simpler methods, the collocation method has not been pursued further.

TABLE 9.  $K_I$  (FINITE ELEMENT) FOR SINGLE EDGE CRACK USING COLLOCATION METHOD. NODAL DISPLACEMENTS OBTAINED FROM APES WITH 3-COLLAPSED TRIANGULAR ELEMENTS. COLLOCATION POINTS ARE EQUALLY SPACED ON  $r=0.01$

No. of Mid=Points Between Nodes	Four-Term Expansion		Eight-Term Expansion	
	General	Mode I ( $a'_s=0$ )	General	Mode I ( $a'_s=0$ )
0			4.90392	4.85093
2			4.82446	4.82966
3				
5	4.82815	4.83417	4.81972	4.82762
9	4.82753	4.83352		
11	4.82743	4.83337		
14	4.82737	4.83322		
19	4.82734	4.83309		

Our second goal in the numerical computation is to assess the accuracy of NASTRAN in linear fracture, using 12-node, isoparametric elements with collapsed triangular elements around a crack tip and to examine the effect of multiple constraints. Normalized stress intensity factors thus obtained are given in Table 10. It indicates a high degree

of accuracy, and the effect of multiple constraints is insignificant. The multiple constraints tend to increase the stress intensity factors slightly. In Table 10, by "No" multiple constraint we mean nodes 2 to 10, Figure 5(a), are free to move in both the local x- and y-directions with respect to node 1, and node 1 has no displacement in the local y-direction due to the symmetry of the problem (mode I crack). The column "Yes" gives results obtained by assuming  $v_1 = v_2 = \dots = v_{10} = 0$  and  $u_1 = u_2 = \dots = u_{10}$ .

TABLE 10.  $K_I$  (NASTRAN)/ $K_I$  (EXACT)

$r_0/a$	0.01		0.015		0.02	
	No	Yes	No	Yes	No	Yes
Center Crack $a/b=0.4, H/b=4.0$ Exact $K_I=1.966$	0.981	1.013	0.982	0.999	0.983	0.994
Double Edge Crack $a/b=0.4, H/b=4.0$ Exact $K_I=2.00$	1.000	1.021	0.998	1.007	0.999	1.002
Single Edge Crack $a/b=0.4, H/b=4.0$ Exact $K_I=3.728$	0.980	1.003	0.980	0.991	0.982	0.988

Another goal in the numerical computation is to compare results using the concept of collapsed triangular elements in APES with results of APES with singular 'core' element around the crack tip. Ratios of  $K_I$  (APES) to  $K_I$  (EXACT) are given in Table 11 for the tension test specimens with  $r_0/a = 0.01$ . Results in the first column of Table 11

are obtained by using three collapsed triangular elements around the crack tip where nodes 1 to 10, Figure 5(a), coincide. All vertical displacements of nodes 1 to 10 are assumed to vanish while they are free to slide with respect to one another in the x-direction. Results in the second column are computed by using a singular 'core' element surrounded by three quadrilateral elements as shown in Figure 5(b) with  $h/r_0 = 6$ . Table 11 shows values of stress intensity factors, obtained by collapsed triangular element, are as accurate as those obtained by using singular 'core' element.

TABLE 11.  $K_I$  (APES)/ $K_I$  (EXACT)

	Collapsed Triangular Elements, Fig. 5(a)	Singular "Core" Elements, Fig. 5(b)
Center Crack $a/b=0.4$ , $H/b=4.0$ Exact $K_I=1.966$	0.998	0.996
Double Edge Crack $a/b=0.4$ , $H/b=4.0$ Exact $K_I=2.00$	1.005	1.011
Single Edge Crack $a/b=0.5$ , $H/b=3.0$ Exact $K_I=5.009$	0.972	0.974

In NASTRAN, it is the user's choice to apply the multiple constraint conditions, equations (27), at the crack tip. But in APES, it is not yet available for the application of multiple constraints. Since the effect of multiple constraints is so small, Table 10, that results from APES with collapsed triangular elements are considered correct even if the multiple constraint conditions (27) are not satisfied.

For the integration of the element stiffness matrices, a 3 x 3 Gaussian quadrature is used in all NASTRAN results in this report while a 4 x 4 Gaussian quadrature is used in APES.

For a mixed mode crack, six collapsed triangular elements shown in Figure 6(a) are used. An effective way to estimate the stress intensity factors is to use  $v(r_0, -\pi)$  for  $K_1$  and  $u(r_0, \pi)$  and  $u(r_0, -\pi)$  for  $K_2$ .

$$\left. \begin{aligned} K_1(\pi) &= \frac{\sqrt{2\pi} \ 2G \ v(r_0, \pi)}{\sqrt{r_0} \ (\kappa+1)} \quad , \quad K_1(-\pi) = \frac{-\sqrt{2\pi} \ 2G \ v(r_0, -\pi)}{\sqrt{r_0} \ (\kappa+1)} \\ K_2(\pi) &= \frac{\sqrt{2\pi} \ 2G \ u(r_0, \pi)}{\sqrt{r_0} \ (\kappa+1)} \quad , \quad K_2(-\pi) = \frac{-\sqrt{2\pi} \ 2G \ u(r_0, -\pi)}{\sqrt{r_0} \ (\kappa+1)} \\ K_1 &= \frac{1}{2} (K_1(\pi) + K_1(-\pi)) \quad , \quad K_2 = \frac{1}{2} (K_2(\pi) + K_2(-\pi)) \end{aligned} \right\} (40)$$

where  $u(r_0, \pi)$  and  $v(r_0, \pi)$  are displacement components of node 26 relative to node 19 in the direction of parallel and normal to the crack face;  $r_0$  is the distance between nodes 26 and 19.  $u(r_0, -\pi)$  and  $v(r_0, -\pi)$  are the same but of node 20 relative to node 1.

For a 45° edge crack shown in Figure 7, NASTRAN results for  $K_1$  and  $K_2$  are tabulated in Table 12 for  $r_0/a=0.01$  and for various other conditions. Again the multiple constraint conditions, namely  $u_1 = u_2 = \dots = u_{19}$  and  $v_1 = v_2 = \dots = v_{19}$ , give little effect on values of  $K_1$  and  $K_2$ . An obliqued edge crack in a rectangular panel under uniform tension is solved by Freese using a modified mapping collocation method [20].  $K_1$  and  $K_2$ , read from Bowie's graphs (Figure 1.16a and 1.16b of

<sup>20</sup>Bowie, O. L., "Solutions of Plane Crack Problems by Mapping Technique," in Mechanics of Fracture, 1, Edited by G. C. Sih, Noordhoff International Publishing, Leyden, The Netherlands, 1973.

[20]), are approximately 1.86 and 0.88 respectively. Numerical results of the same problem computed by APES, using special crack tip elements and various idealizations, are given in Figure 12 of [16].

TABLE 12.  $K_1$  AND  $K_2$  FOR 45° EDGE CRACK BY NASTRAN

B.C.	Integration	Multiple Constraint	$K_1$	$K_2$
1	3 x 3	No	1.89	0.95
1	3 x 3	Yes	1.89	0.96
1	4 x 4	No	1.83	0.92
2	4 x 4	Yes	1.84	0.93

#### THE STABILITY OF COLLAPSED TRIANGULAR ELEMENTS

In a recent report by Hussain and Lorensen [21], it was found that a slight perturbation in placing the mid-side node opposite to the crack tip for a collapsed 8-node, quadrilateral element led to unstable results in stress intensity factors. This instability can be shown in the collapsed 12-node, quadrilateral element if one or both middle nodes of the side opposite to the crack tip are slightly perturbed from their nominal positions.

Let node 5 be perturbed as shown in Figure 8. Denoting the perturbed quantities with an asterix, we have

<sup>16</sup>Gifford, L. N., "Apes - Second Generation Two-Dimensional Fracture Mechanics and Stress Analysis by Finite Elements," Naval Ship Research and Development Center, Report 4799, December 1975.

<sup>20</sup>Bowie, O. L., "Solutions of Plane Crack Problems by Mapping Technique," in Mechanics of Fracture, 1, Edited by G. C. Sih, Noordhoff International Publishing, Leyden, The Netherlands, 1973.

<sup>21</sup>Hussain, M. A. and Lorensen, W. E., "Isoparametric Elements As Singular Elements for Crack Problems," Watervliet Arsenal Technical Report, to be published.



$$\left. \begin{aligned} x_5^*/\ell &= \frac{2 + \cos\alpha}{3} + \epsilon \\ y_5^*/\ell &= \frac{\sin\alpha}{3} + \epsilon' \end{aligned} \right\} \quad (41)$$

A general point (x,y) given by equation (18) will be displaced at

$$x^*/\ell = \frac{1}{8} (1+\xi)^2 [(1-\eta) + (1+\eta)\cos\alpha] + \epsilon \frac{9}{32} (1+\xi)(1-\eta^2)(1-3\eta) \quad (42)$$

$$y^*/\ell = \frac{1}{8} (1+\xi)^2 (1+\eta)\sin\alpha + \epsilon' \frac{9}{32} (1+\xi)(1-\eta^2)(1-3\eta) \quad (43)$$

Along the line  $\eta = -1/3$ , and replacing  $y^*$  with  $r \sin\theta$  in (40), we have

$$1 + \xi = \frac{3}{\sin\alpha} \left[ -1 + \left( 1 + \frac{r}{\ell} \frac{4\sin\theta\sin\alpha}{3\epsilon'^2} \right)^{1/2} \right] \quad (44)$$

Since  $(1+\xi)$  is a common factor in displacement components, equations (28) and (29), it is seen that the singularity required, for the crack problems disappears along at least the ray  $\eta = -1/3$  in the collapsed triangular case.

As a numerical example, the central crack tension specimen of Figure 3(a) is again used. If the idealization remained the same as shown in Figure 4, except that the collapsed elements of Figure 5 were replaced by those of Figure 8(b) (where nodal points 20, 21, 23, 24, 26 and 27 are on a circular arc), the computed stress intensity factor changed from its almost exact value  $K_I = 1.962$  to  $K_I = 1.421$  (nearly 30% error). If only nodal points 26 and 27 were perturbed to their new locations in Figure 8(b), the stress intensity factor would become  $K_I = 1.457$  (a 26% error).

## CONCLUSIONS

By a simple manner, the 12-node isoparametric elements can be used to form a singular element for two-dimensional, elastic, fracture mechanics analysis. The elements have been successfully implemented in NASTRAN, which can now be more efficiently used for more accurate prediction of stress intensity factors of complicated crack problems. The middle nodes of the side opposite to a crack tip in a collapsed triangular element should be accurately located to avoid unstable results. The extension of collapsed triangular elements as singular elements to three-dimensional brick elements can be easily done as in [9,10].

---

<sup>9</sup>Barsoum, R. S., "On the Use of Isoparametric Finite Elements in Linear Fracture Mechanics," International Journal for Numerical Methods in Engineering, Vol. 10, 1976.

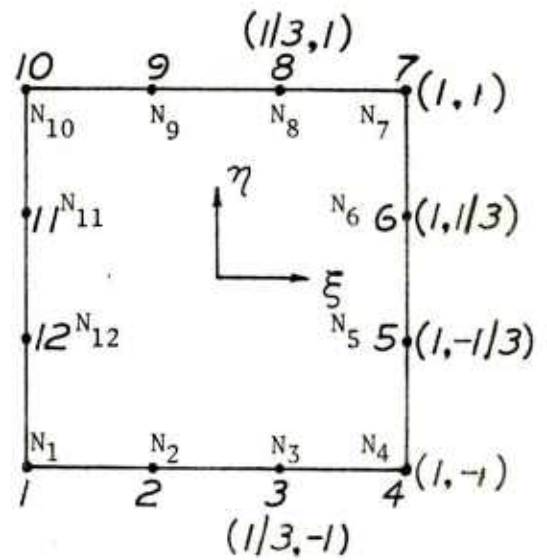
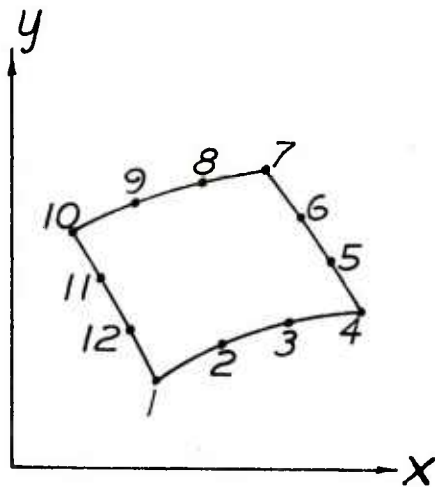
<sup>10</sup>Hussain, M. A., Lorensen, W. E., and Pflieg1, G., "The Quarter-Point Quadratic Isoparametric Element As a Singular Element for Crack Problems," NASA TM-X-3428, 1976, p. 419.

## REFERENCES

1. Swedlow, J. L., Williams, M. L., and Yang, W. H., "Elasto-Plastic Stresses and Strains in Cracked Plates," Proceedings First International Conference on Fracture, 1, p. 259, 1966.
2. Kobayashi, A. S., Maiden, D. E. and Simon, B. J., "Application of the Method of Finite Element Analysis to Two-Dimensional Problems in Fracture Mechanics," ASME 69-WA/PVP-12 (1969).
3. Chan, S. K., Tuba, I. S. and Wilson, W. K., "On Finite Element Method in Linear Fracture Mechanics," Engineering Fracture Mechanics, 2, p. 1, 1970.
4. Wilson, W. K., "Combined Mode Fracture Mechanics," Ph.D. Dissertation, University of Pittsburgh, 1969.
5. Tracey, D. M., "Finite Elements for Determination of Crack Tip Elastic Stress Intensity Factors," Engineering Fracture Mechanics, Vol. 3, 1971.
6. Blackburn, W. S., "Calculation of Stress Intensity Factors at Crack Tips Using Special Finite Elements," The Mathematics of Finite Elements and Applications, Brunel University, 1973.
7. Benzley, S. E. and Beisinger, A. E., "Chiles - A Finite Element Computer Program That Calculates the Intensities of Linear Elastic Singularities," Sandia Laboratories, Technical Report SLA-73-0894, 1973.
8. Henshell, R. D., and Shaw, K. G., "Crack Tip Finite Elements Are Unnecessary," International Journal for Numerical Methods in Engineering, Vol. 9, 1975.

9. Barsoum, R. S., "On the Use of Isoparametric Finite Elements in Linear Fracture Mechanics," *International Journal for Numerical Methods in Engineering*, Vol. 10, 1976.
10. Hussain, M. A., Lorensen, W. E., and Pflieg1, G., "The Quarter-Point Quadratic Isoparametric Element As a Singular Element for Crack Problems," NASA TM-X-3428, 1976, p. 419.
11. Zienkiewicz, O. O., The Finite Element Method in Engineering Science, McGraw Hill, London, 1971.
12. Barsoum, R. S., "Triangular Quarter-Point Elements As Elastic and Perfectly-Plastic Crack Tip Elements," *International Journal for Numerical Methods in Engineering*, Vol. 11, 1977.
13. Williams, M. L., "On the Stress Distribution at the Base of a Stationary Crack," *Journal of Applied Mechanics*, Vol. 24, 1957.
14. Tracey, D. M., "Discussion of 'On the Use of Isoparametric Finite Elements in Linear Fracture Mechanics' by R. S. Barsoum", *Int. Journal for Numerical Methods in Engineering*, Vol. 11, 1977.
15. Barsoum, R. S., "Author's Reply to the Discussion by Tracey," *Int. Journal for Numerical Methods in Engineering*, Vol. 11, 1977.
16. Gifford, L. N., "Apes - Second Generation Two-Dimensional Fracture Mechanics and Stress Analysis by Finite Elements," Naval Ship Research and Development Center, Report 4799, December 1975.
17. Isida, M., "Analysis of Stress Intensity Factors for the Tension of a Centrally Cracked Strip with Stiffened Edges," *Engineering Fracture Mechanics*, Vol. 5, 1973.

18. Brown, W. F., and Srawley, J. E., "Plane Strain Crack Toughness Testing of High Strength Metallic Materials," ASTM STP-410, 1966.
19. Tada, H., Paris, P. and Irwin, G., The Stress Analysis of Cracks Handbook, Del Research Corp., 1973.
20. Bowie, O. L., "Solutions of Plane Crack Problems by Mapping Technique," in Mechanics of Fracture, 1, Edited by G. C. Sih, Noordhoff International Publishing, Leyden, The Netherlands, 1973.
21. Hussain, M. A. and Lorensen, W. E., "Isoparametric Elements As Singular Elements for Crack Problems," Watervliet Arsenal Technical Report, to be published.



$$N_1 = \frac{1}{32} (1-\eta) (1-\xi) [-10+9(\xi^2+\eta^2)]$$

$$N_2 = \frac{9}{32} (1-\eta) (1-\xi^2) (1-3\xi)$$

$$N_3 = \frac{9}{32} (1-\eta) (1-\xi^2) (1+3\xi)$$

$$N_4 = \frac{1}{32} (1-\eta) (1+\xi) [-10+9(\xi^2+\eta^2)]$$

$$N_5 = \frac{9}{32} (1+\xi) (1-\eta^2) (1-3\eta)$$

$$N_6 = \frac{9}{32} (1+\xi) (1-\eta^2) (1+3\eta)$$

$$N_7 = \frac{1}{32} (1+\eta) (1+\xi) [-10+9(\xi^2+\eta^2)]$$

$$N_8 = \frac{9}{32} (1+\eta) (1-\xi^2) (1+3\xi)$$

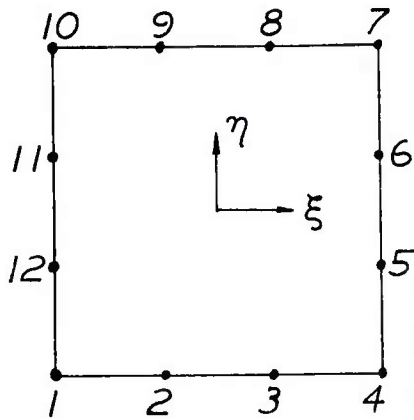
$$N_9 = \frac{9}{32} (1+\eta) (1-\xi^2) (1-3\xi)$$

$$N_{10} = \frac{1}{32} (1+\eta) (1-\xi) [-10+9(\xi^2+\eta^2)]$$

$$N_{11} = \frac{9}{32} (1-\xi) (1-\eta^2) (1+3\eta)$$

$$N_{12} = \frac{9}{32} (1-\xi) (1-\eta^2) (1-3\eta)$$

Figure 1. Shape Functions and Numbering Sequence For a 12-Node Quadrilateral Element.



NODE	$x/l$	$y/l$
1	0	0
2	$\cos\beta/9$	$\sin\beta/9$
3	$4\cos\beta/9$	$4\sin\beta/9$
4	$\cos\beta$	$\sin\beta$
5	$(2\cos\beta+\cos\alpha)/3$	$(2\sin\beta+\sin\alpha)/3$
6	$(\cos\beta+2\cos\alpha)/3$	$(\sin\beta+2\sin\alpha)/3$
7	$\cos\alpha$	$\sin\alpha$
8	$4\cos\alpha/9$	$4\sin\alpha/9$
9	$\cos\alpha/9$	$\sin\alpha/9$
10	0	0
11	0	0
12	0	0

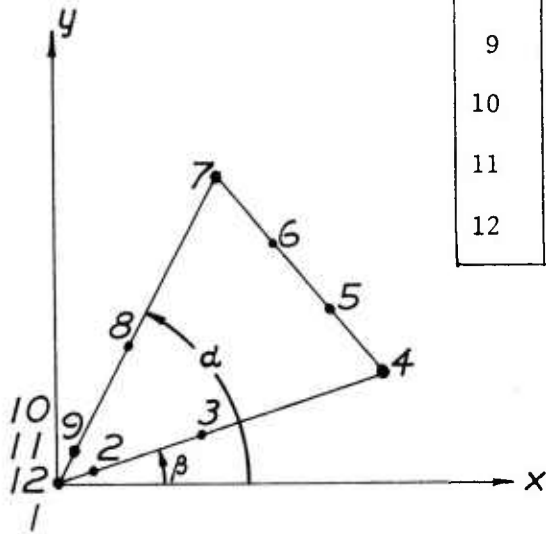
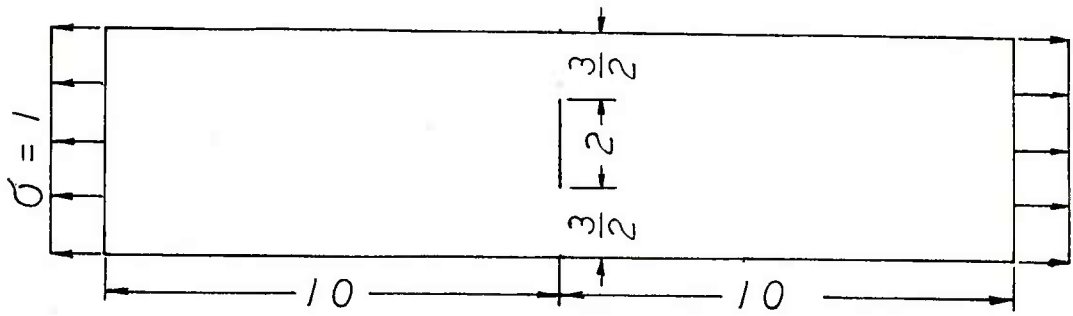
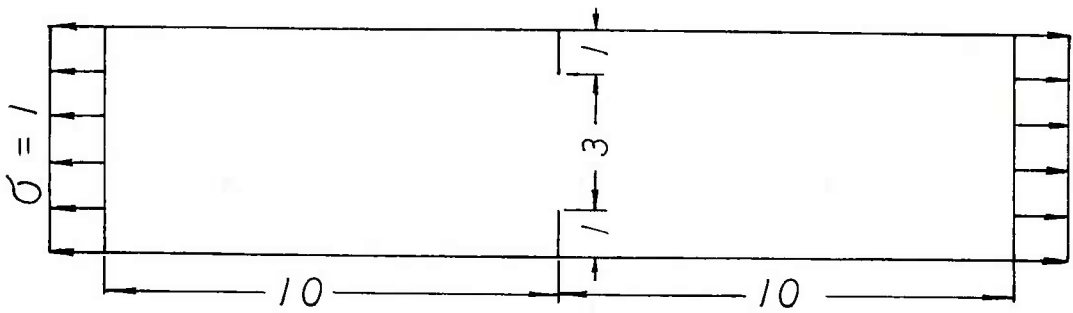


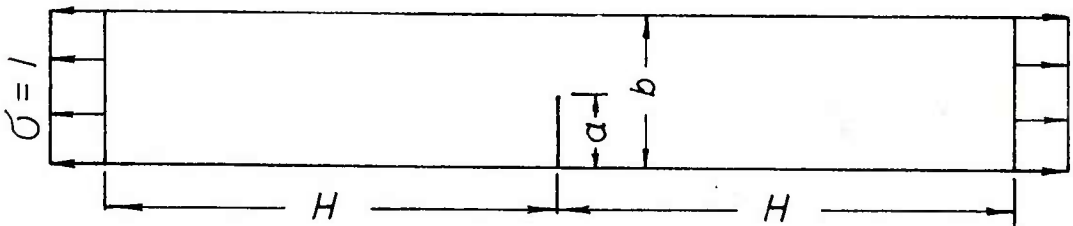
Figure 2. A Normalized Square in  $(\xi, \eta)$  Plane Mapped Into a Collapsed Triangular Element in  $(x, y)$  Plane with the side  $\xi = -1$  Degenerated into a Point at the Crack Tip.



(a) Center Crack



(b) Double-Edge Crack



(c) Single-Edge Crack

Figure 3. Three Tension Test Specimens.



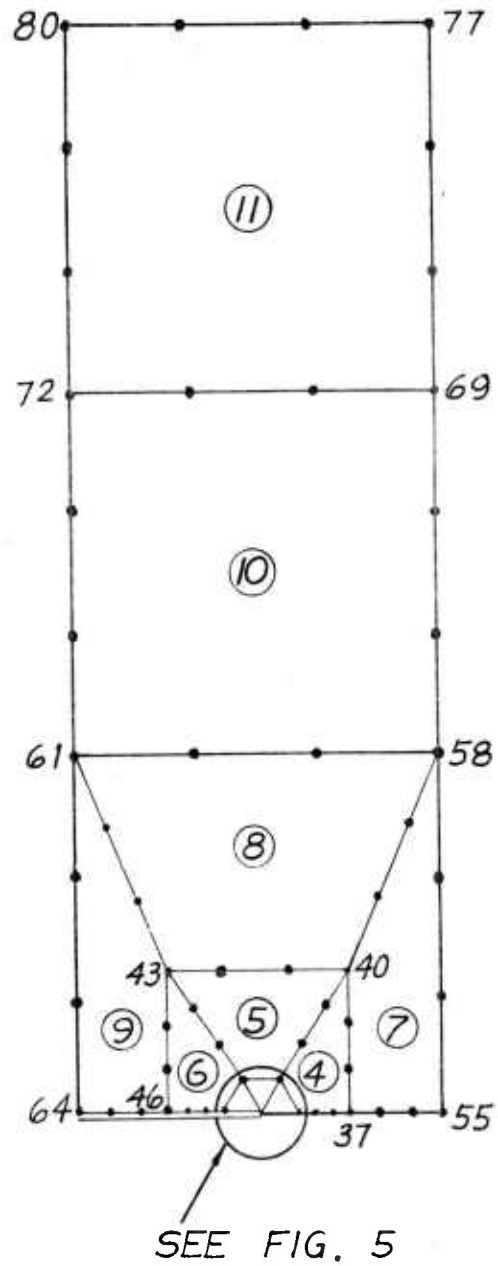


Figure 4. Idealization of a Half of the Single-Edge Cracked Tension Specimen.

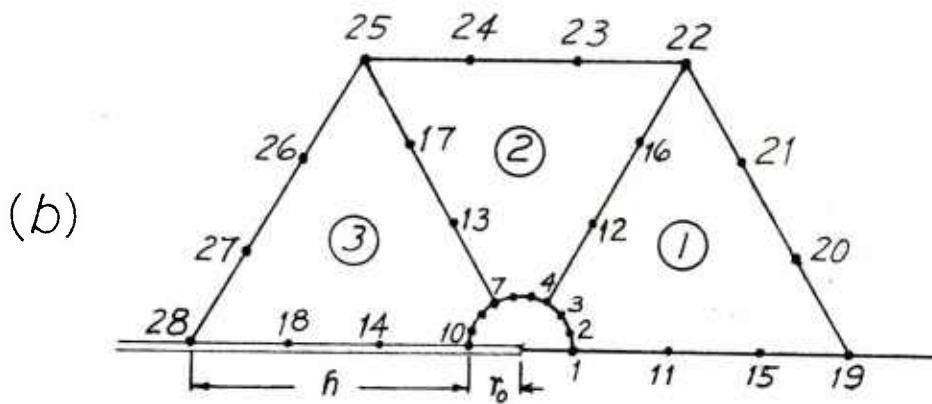
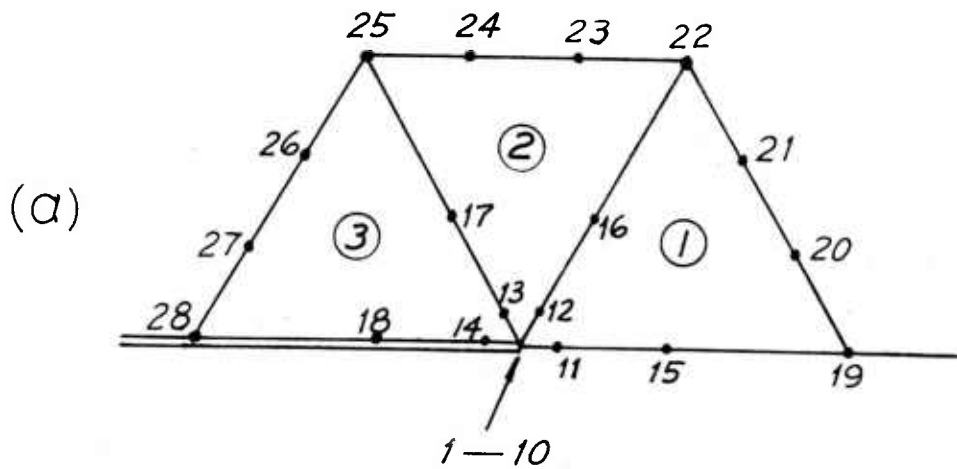


Figure 5(a). Three Collapsed Triangular Elements Surrounding a Mode I Crack Tip.  
 (b). Special Core Element and Three Quadrilateral Elements Surrounding a Mode I Crack Tip.

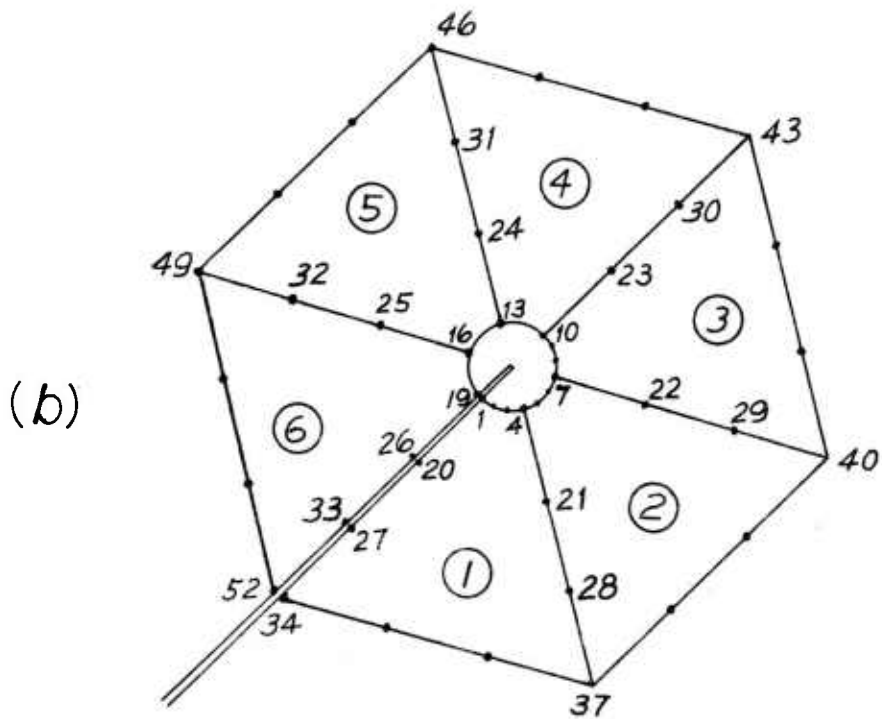
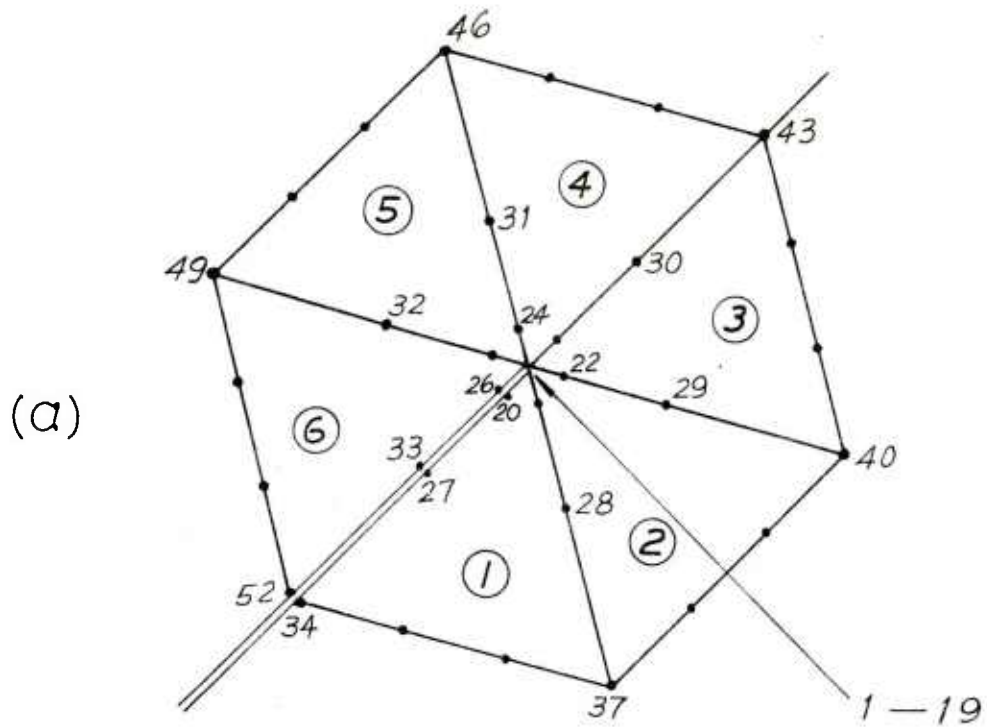


Figure 6(a). Six Collapsed Triangular Elements Surrounding a Mixed Mode Crack Tip.  
 (b). Special Core Element and Six Quadrilateral Elements Surrounding a Mixed Mode Crack Tip.

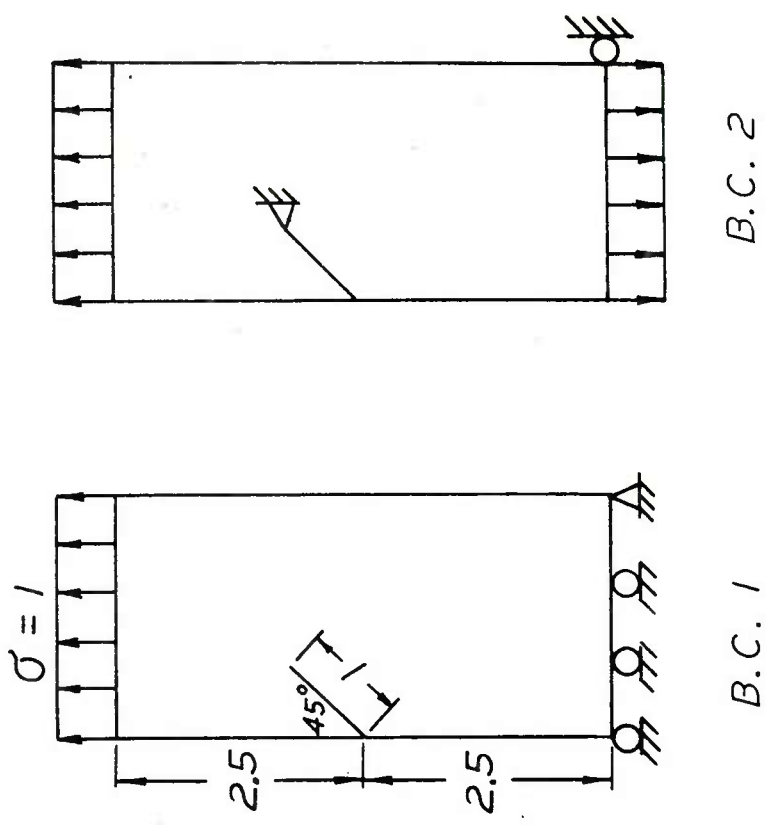
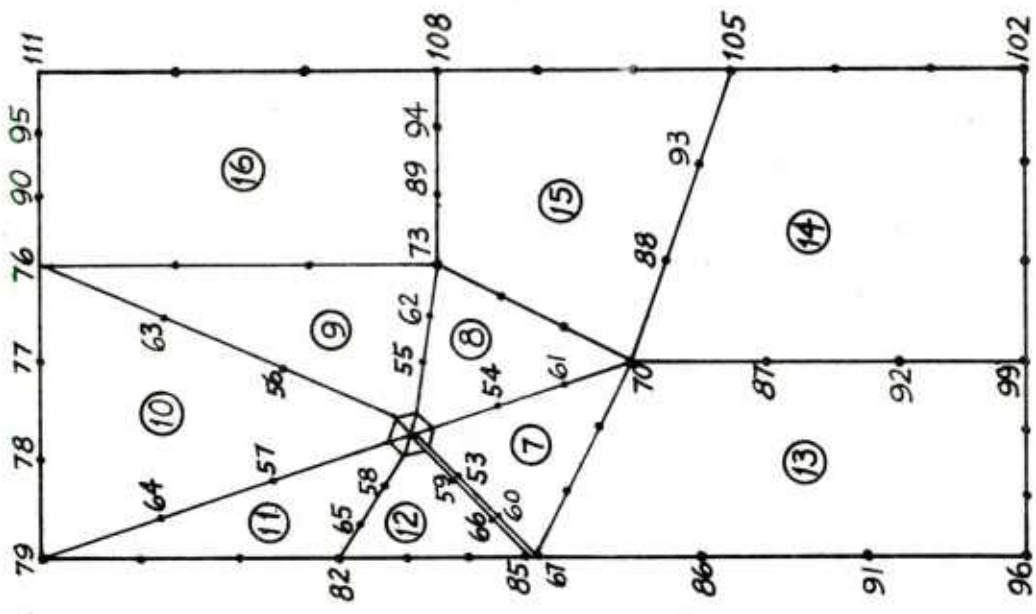


Figure 7. Idealization of a 45-Degree Slant Edge Cracked Panel in Tension.

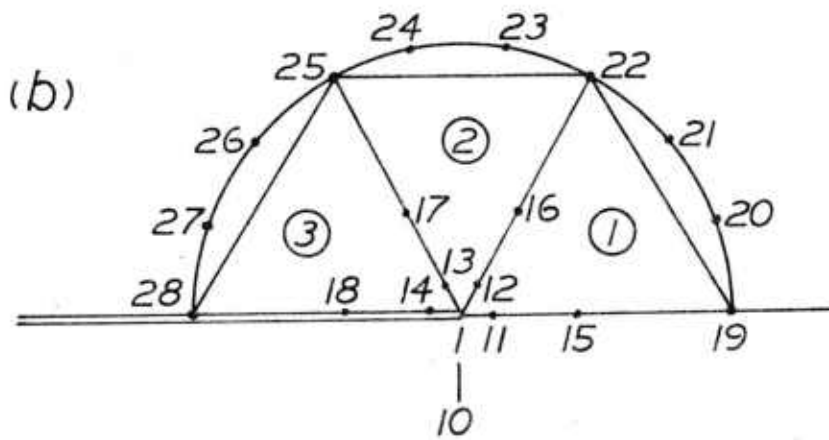
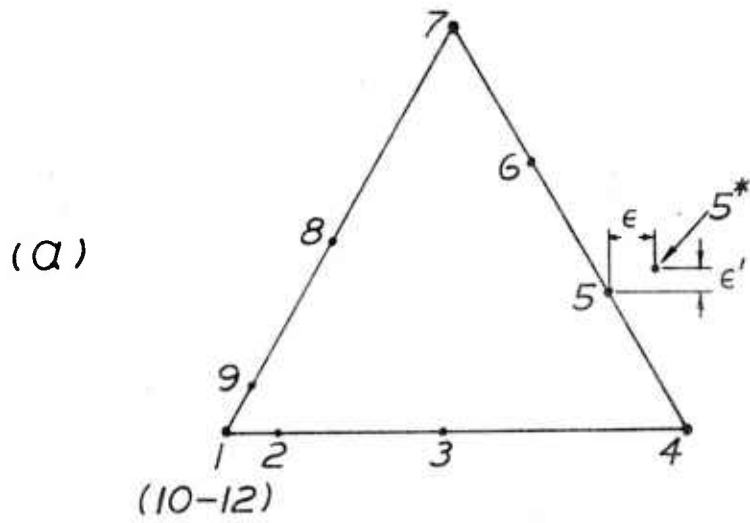


Figure 8(a). Node 5 Perturbed to 5\*.  
 (b). Nodes 20, 21, 23, 24, 26, 27 Perturbed From Their Nominal Positions.

WATERVLIET ARSENAL INTERNAL DISTRIBUTION LIST

	<u>NO. OF COPIES</u>
COMMANDER	1
DIRECTOR, BENET WEAPONS LABORATORY	1
CHIEF, DEVELOPMENT ENGINEERING BRANCH	1
ATTN: DRDAR-LCB-DA	1
-DM	1
-DP	1
-DR	1
-DS	1
-DC	1
CHIEF, ENGINEERING SUPPORT BRANCH	1
CHIEF, RESEARCH BRANCH	2
ATTN: DRDAR-LCB-RA	1
-RC	1
-RM	1
-RP	1
TECHNICAL LIBRARY	5
TECHNICAL PUBLICATIONS & EDITING UNIT	2
DIRECTOR, OPERATIONS DIRECTORATE	1
DIRECTOR, PROCUREMENT DIRECTORATE	1
DIRECTOR, PRODUCT ASSURANCE DIRECTORATE	1

NOTE: PLEASE NOTIFY DIRECTOR, BENET WEAPONS LABORATORY, ATTN:  
DRDAR-LCB-TL, OF ANY REQUIRED CHANGES.

EXTERNAL DISTRIBUTION LIST (CONT)

	<u>NO. OF COPIES</u>		<u>NO. OF COPIES</u>
COMMANDER US ARMY RESEARCH OFFICE P.O. BOX 12211 RESEARCH TRIANGLE PARK, NC 27709	1	COMMANDER DEFENSE DOCU CEN ATTN: DDC-TCA CAMERON STATION ALEXANDRIA, VA 22314	12
COMMANDER US ARMY HARRY DIAMOND LAB ATTN: TECH LIB 2800 POWDER MILL ROAD ADELPHIA, MD 20783	1	METALS & CERAMICS INFO CEN BATTELLE COLUMBUS LAB 505 KING AVE COLUMBUS, OHIO 43201	1
DIRECTOR US ARMY INDUSTRIAL BASE ENG ACT ATTN: DRXPE-MT ROCK ISLAND, IL 61201	1	MPDC 13919 W. BAY SHORE DR. TRAVERSE CITY, MI 49684	1
CHIEF, MATERIALS BRANCH US ARMY R&S GROUP, EUR BOX 65, FPO N.Y. 09510	1		
COMMANDER NAVAL SURFACE WEAPONS CEN ATTN: CHIEF, MAT SCIENCE DIV DAHLGREN, VA 22448	1		
DIRECTOR US NAVAL RESEARCH LAB ATTN: DIR, MECH DIV CODE 26-27 (DOC LIB) WASHINGTON, D.C. 20375	1 1		
COMMANDER WRIGHT-PATTERSON AFB ATTN: AFML/MXA OHIO 45433	2		
NASA SCIENTIFIC & TECH INFO FAC P.O. BOX 8757, ATTN: ACQ BR BALTIMORE/WASHINGTON INTL AIRPORT MARYLAND 21240	1		

NOTE: PLEASE NOTIFY COMMANDER, ARRADCOM, ATTN: BENET WEAPONS LABORATORY, DRDAR-LCB-TL, WATERVLIET ARSENAL, WATERVLIET, N.Y. 12189, OF ANY REQUIRED CHANGES.

EXTERNAL DISTRIBUTION LIST

	<u>NO. OF COPIES</u>		<u>NO. OF COPIES</u>
ASST SEC OF THE ARMY RESEARCH & DEVELOPMENT ATTN: DEP FOR SCI & TECH THE PENTAGON WASHINGTON, D.C. 20315	1	COMMANDER US ARMY TANK-AUTMV R&D COMD ATTN: TECH LIB - DRDTA-UL MAT LAB - DRDTA-RK WARREN, MICHIGAN 48090	1 1
COMMANDER US ARMY MAT DEV & READ. COMD ATTN: DRCDE 5001 EISENHOWER AVE ALEXANDRIA, VA 22333	1	COMMANDER US MILITARY ACADEMY ATTN: CHMN, MECH ENGR DEPT WEST POINT, NY 10996	1
COMMANDER US ARMY ARRADCOM ATTN: DRDAR-TSS DRDAR-LCA (PLASTICS TECH EVAL CEN) DOVER, NJ 07801	2 1	COMMANDER REDSTONE ARSENAL ATTN: DRSMI-RB DRSMI-RRS DRSMI-RSM ALABAMA 35809	2 1 1
COMMANDER US ARMY ARRCOM ATTN: DRSAR-LEP-L ROCK ISLAND ARSENAL ROCK ISLAND, IL 61299	1	COMMANDER ROCK ISLAND ARSENAL ATTN: SARRI-ENM (MAT SCI DIV) ROCK ISLAND, IL 61202	1
DIRECTOR BALLISTICS RESEARCH LAB ATTN: DRDAR-TSB-S ABERDEEN PROVING GROUND, MD 21005	1	COMMANDER HQ, US ARMY AVN SCH ATTN: OFC OF THE LIBRARIAN FT RUCKER, ALABAMA 36362	1
COMMANDER US ARMY ELECTRONICS COMD ATTN: TECH LIB FT MONMOUTH, NJ 07703	1	COMMANDER US ARMY FGN SCIENCE & TECH CEN ATTN: DRXST-SD 220 7TH STREET, N.E. CHARLOTTESVILLE, VA 22901	1
COMMANDER US ARMY MOBILITY EQUIP R&D CCMD ATTN: TECH LIB FT BELVOIR, VA 22060	1	COMMANDER US ARMY MATERIALS & MECHANICS RESEARCH CENTER ATTN: TECH LIB - DRXMR-PL WATERTOWN, MASS 02172	2

NOTE: PLEASE NOTIFY COMMANDER, ARRADCOM, ATTN: BENET WEAPONS LABORATORY, DRDAR-LCB-TL, WATERVLIET ARSENAL, WATERVLIET, N.Y. 12189, OF ANY REQUIRED CHANGES.